Title: Interhemispheric Connectivity Supports Load-Dependent Working Memory Maintenance for Complex Visual Stimuli

Short Title: Connectivity and Working Memory Maintenance

Key Words: Working Memory, Delay Activity, Maintenance, Interference, Connectivity

Author names and affiliations:
Chelsea Reichert Plaska[1,2]
Jefferson Ortega[1]
Bernard A. Gomes[3]
Timothy M. Ellmore[1,2]

[1]The Behavioral and Cognitive Neuroscience Program, CUNY Graduate Center, [2]Department of Psychology, The City College of New York, [3]Cedars-Sinai Medical Center, Los Angeles, CA

Corresponding Author: Timothy M. Ellmore, Ph.D. (tellmore@ccny.cuny.edu)

Permanent Address: Department of Psychology, The City College of New York, North Academic Center, 160 Convent Avenue, New York, NY 10031

Abstract

An open question in the working memory (WM) field is how information is kept online during the WM delay period. Maintenance of simple stimuli in WM is supported by connectivity between frontal and parietal brain regions. How does delay period activity and connectivity support WM of complex stimuli? Twenty-two participants completed a modified Sternberg WM task with complex stimuli and were told to remember either 2 (low-load) or 5 (high-load) scenes while 32-channel scalp EEG was recorded. During the 6-sec delay period 6 phase-scrambled scenes were presented, which served as interference. While increasing the WM load, particularly with complex stimuli, places a greater demand on attentional resources, interfering stimuli may hijack the available resources. This was confirmed in the examination of theta and alpha amplitude, as amplitude was reduced for the high WM load as compared with the low WM load across frontal, central, and parietal regions. Delay period connectivity was assessed with phase-locking value (PLV). We identified 3 supporting networks that facilitated performance for the low-load condition: 1) increased PLV between left frontal and right posterior temporal in the theta and alpha bands; 2) increased PLV between right anterior temporal and left central in the alpha and lower beta bands; and 3) increased PLV between left anterior temporal and left posterior temporal in theta, alpha, and lower beta bands for the low-load condition. These results suggest that these brain networks facilitated the low-load WM by filtering of interference and the use of verbal rehearsal during the delay period.

Impact Statement:

Although, studies of working memory maintenance with simple stimuli have suggested a role of frontal-parietal networks in supporting maintenance, the current study suggests that maintenance of complex visual stimuli with interference present is supported by interhemispheric frontal-posterior temporal and intrahemispheric left temporal region connectivity. These networks support maintenance by filtering of the interfering stimuli, which facilitates the use of verbal rehearsal strategies during the delay period.

1 Introduction

1.1 Visual Working Memory Maintenance

Visual working memory encompasses temporary storage of visually presented information. Research on the neural correlates of visual working memory (WM) has often focused on simple and easy-to-name stimuli, like shapes or line drawings, with few studies examining WM for complex visual stimuli. Adding complexity to stimuli may impact how much information is able to be maintained in WM (Alvarez & Cavanagh, 2004; Awh et al., 2007) and what underlying brain regions support them. For example, using a complex stimulus such as a natural scene puts a greater demand on attention than a simple line drawing because it requires the perception and combination of more features (Lavie et al., 2004). Complexity also impacts executive resources available to maintain stimuli as well as block out irrelevant information that could interfere with maintenance (Lavie, 1995). These attentional processes rely on prefrontal brain regions and frontoparietal networks (Gruber & Goschke, 2004). Adding complexity may also modulate the ability to recode the images and use rehearsal (Baddeley, 2010, 2012; Baddeley & Hitch, 1974). Easy-to-name stimuli would rely on brain regions traditionally implicated in rehearsal, - such as left-hemisphere speech areas (Gruber, 2001; Smith & Jonides, 1998), whereas difficult-to-name stimuli may rely on processes such as attentional refreshing (Cowan et al., 2005) that implicate prefrontal regions. *This leaves open the question of how is complex visual information represented in the brain and what networks support maintenance of this type of information?*

Examination of the neural activity during the delay period of a WM task, when task-related information is being maintained but is no longer presented, is called delay activity (Sreenivasan & D'Esposito, 2019). Delay activity is often examined in the absence of visual stimuli by the presentation of a blank screen or a fixation cross. During these periods attention is assumed to be fully engaged on the WM task and is represented by increased and sustained

delay activity in the prefrontal cortex and parietal regions in animals and humans (Constantinidis et al., 2018; Goldman-Rakic, 1995; Sreenivasan et al., 2014). Increased alpha power and event-related synchronization using EEG have been identified as the critical correlate of working memory maintenance during the delay period in posterior temporal-parietal (Feredoes et al., 2011; Sarnthein et al., 1998; Scheeringa et al., 2009) and superior parietal regions (Jensen et al., 2002; Palva et al., 2010), which likely reflects suppression of potentially interfering neural processes (Jensen & Mazaheri, 2010) or external distraction (Bonnefond & Jensen, 2012). Increases in theta band activity (Jensen & Tesche, 2002) and beta activity (Jensen & Mazaheri, 2010) in frontal regions have also been observed during maintenance, which reflect attentional processes and control over maintained stimuli, respectively. The theta, alpha, and beta frequency oscillations all show increases in delay activity with increasing working memory load (Jensen & Tesche, 2002; Mazaheri & Jensen, 2010; Pavlov & Kotchoubey, 2020; Scheeringa et al., 2009; Tuladhar et al., 2007). Gamma band increases have also been implicated in WM, especially with regards to encoding of material (Mainy et al., 2007; Pavlov & Kotchoubey, 2020).

Similar to increased delay activity in lower frequency bands being associated with increased WM load (see (Pavlov & Kotchoubey, 2020), increased functional connectivity has also been reported (Payne & Kounios, 2009; Tóth et al., 2012; Zakrzewska & Brzezicka, 2014; Zhang et al., 2016) during WM maintenance. Connectivity is a method that is applied to both EEG and fMRI to estimate the degree of interaction between two brain regions (Fell & Axmacher, 2011; Fries, 2005) as well as provide insight into brain networks the underly WM maintenance (Gazzaley et al., 2004; Zhang et al., 2016). In addition to increased activity in these regions during the delay period, a frontoparietal network has been identified as supporting WM maintenance both in fMRI (Bollinger et al., 2010; Hampson et al., 2006) and EEG (Babiloni et al., 2004; Palva et al., 2010). Increased connectivity in the lower frequency bands, such as theta and alpha are attributed to attentional processes (Palva et al., 2010; Zhang et al., 2016), whereas higher frequency bands such as beta and gamma are attributed to stimulus

representation (Palva et al., 2010). In fact, increases in right hemisphere frontoparietal connections is implicated in sustained attention during WM (Coull et al., 1996). Additionally, connectivity between frontal - visual regions and frontal - posterior temporal regions has also been implicated in supporting maintenance and executive control over maintenance (Daume et al., 2017; Gruber & Goschke, 2004; Rezayat et al., 2021).

1.2 Attention and Maintenance

Attention plays a different role at each stage of WM, including selective attention towards encoding and focused attention on task stimuli during maintenance (Gazzaley & Nobre, 2012). Information that captures attention during encoding, such as target stimuli, is prioritized over information that is to be ignored (Gazzaley & Nobre, 2012), which suggests that studying delay activity with a blank screen is sufficient for understanding the neural pinning's of WM. However, research has shown that distracting information can automatically capture attention along with task-related information (Lavie & Cox, 1997). Therefore examining distraction during WM can provide insight into how attention supports maintenance of relevant information while filtering out irrelevant information through the examination of connectivity between prefrontal and posterior brain areas (Gazzaley & Nobre, 2012). There are two experimental manipulations that are commonly employed to study attention in WM, the presentation of task-irrelevant information that is intended to be ignored (Cowan, 2011) or with the addition of a secondary task (Morey & Cowan, 2005; Ricker et al., 2010) that is not related to the primary task goal. Both methods of external interference can negatively impact performance (Chen & Cowan, 2009; Clapp et al., 2010).

The impact of distractors is related to the attentional demand of the task, which is manipulated by either increasing the amount of information to be maintained or the complexity of the stimuli (Alvarez & Cavanagh, 2004; Chen & Cowan, 2009; Simon et al., 2016; Xu & Chun, 2006). As task demand increases, all attentional resources available for processing of the stimuli are used automatically in the early stages of attention (Lavie, 1995). So according to

Load Theory, once the perceptual load (i.e., amount of perceptual processing required for a stimulus) has reached capacity, there should be no resources available to process other stimuli that may be presented, such a distractor (Lavie, 1995; Lavie & Cox, 1997; Simon et al., 2016). Studies have found that increased task demands (e.g., increased load) results in reduced distractor processing (Sörqvist et al., 2016) which suggests that increased distractor processing is more likely to occur with the addition of a dual-task or whether or not a distractor was expected (SanMiguel et al., 2008). A number of studies have found that distraction influences connectivity in the attention networks that support encoding and maintenance (Greene & Soto, 2014). Specifically, interference during maintenance has been found to disrupt the connectivity between the prefrontal regions and visual regions (Yoon et al., 2006) as well as prefrontal and parietal regions (Greene & Soto, 2014). These long-range connections are important for the top-down control of WM (Gazzaley & Nobre, 2012; Von Stein & Sarnthein, 2000) and allocation of attentional resources (Sauseng et al., 2005), processes that are particularly important with increased task demands.

1.3 The Present Study

The goal of the present study was to identify the neural and connectivity patterns that support WM maintenance for complex visual stimuli. The hallmark pattern of sustained delay activity has been challenged in recent years (Constantinidis et al., 2018; Sreenivasan et al., 2014; Sreenivasan & D'Esposito, 2019). Work from our lab provides support for this hallmark pattern, but questions about how complex visual stimuli and longer delay periods may influence this pattern remain unanswered (Ellmore et al., 2017; Plaska et al., 2021). Moreover, examining how maintenance and attention are reflected in delay activity is of critical importance to understanding how visual information is successfully maintained until it is retrieved and what delay activity represents (Sreenivasan & D'Esposito, 2019). Namely, attention is presumed to be engaged throughout the delay and it is often used to explain the established patterns of delay activity (e.g., increased alpha activity, see Jensen and Mazaheri (2010)). *What happens*

when the demand on attention is increased with complex visual stimuli and increasing load? How does this change when the delay period contains interfering stimuli, as compared with a standard blank delay period? Additionally, while many EEG delay activity and connectivity studies focus exclusively on frontoparietal interactions (Sauseng et al., 2005), analysis of widespread connectivity is critical for understanding how complex visual stimuli are maintained because complex stimuli may involve additional maintenance processes such associations with semantic knowledge (Von Stein & Sarnthein, 2000) that simple stimuli may not require, which may be associated with more posterior regions.

The present study was designed to examine how increasing the working memory load influences delay activity patterns for complex visual stimuli. Participants maintained either 2 or 5 complex stimuli during the delay period while looking at a perceptual baseline of 6 phase-scrambled stimuli that lacked semantic content. Participants were not required to remember the perceptual baseline, so it also served as visual interference. Delay activity is often examined during a period with no visual input or a simple fixation with sparse visual input (e.g., a fixation cross on a blank screen), so the hypothesis is that introducing perceptually similar visual information during the delay period will engage attention and distract from maintenance. We predict that if delay activity is a signature of maintenance and attention is crucial for successful maintenance, the introduction of interference will be reflected in delay activity and have an impact on performance. When there is a greater demand on attentional resources, such as with the maintenance of a high WM load, there are fewer resources available to process the interfering stimuli. It is predicted that if the low-load WM condition requires fewer attentional resources to maintain, there will be attentional resources available to process the interfering stimuli and no resources leftover for the high-load condition. As a result, there will be a greater reduction in delay activity, especially in frontal regions critical for attention and maintenance and performance will be negatively impacted. Additionally, it is predicted that there will be increased

frontoparietal connectivity during the delay period to support filtering of interference, which will be greater for the high-load as compared with the low-load condition.

2 Methods

2.1 *Participants*. The study was approved by the City University of New York Integrative Institutional Review Board (CUNY IRB). These data were collected as part of a simultaneous EEG/MRI study, so all participants completed an MRI safety questionnaire; after review and approval by the MRI director, they signed the informed consent form. The focus of this analysis is on the EEG data. The study consisted of 24 subjects that signed the informed consent and completed the study. A total of 2 subjects were excluded from all analyses because of unusable EEG data or failure to complete both conditions (i.e., fell asleep during one of the task conditions) which left a final sample of 22 subjects (12 females, age range 18 to 54, mean age 24.95 years, SD = 8.57). Three of these participants mixed up the button responses during one of the WM conditions; therefore, all analyses were repeated excluding these participants to confirm that they did not influence the behavioral results.

Task and Set-up. The present study employed a modified version of the Sternberg WM task (Sternberg, 1966) with a classic load manipulation of low (2 stimuli) and high (5 stimuli) working memory loads . Participants completed 50 trials of each condition in a randomized order. Approximately 10-minutes later participants completed an immediate recognition task. Before going to the MRI scanner, participants completed practice working memory trials and recognition trials (3 for each condition) in the MRI control room. Before completing each task condition, participants were read the same instructions that were given to them during the practice.

The Sternberg WM task is great for studying load manipulations and attention during maintenance because this task requires selective attention towards presented stimuli throughout the stages of working memory (Gazzaley & Nobre, 2012). The load manipulation

ensures that there are different levels of task demand on attention (Lavie, 2005). This task is also ideal for EEG analysis of memory as the task is organized by encoding, maintenance, and retrieval.

The task consisted of an encoding phase (*Figure 1*; 2 or 5 stimuli presented for 1400 ms each), a maintenance or delay period (6000 ms), a probe choice task (1400 ms) followed by a jitter period with a blank screen (approx. 3000 ms). During the delay period 6 phase-scrambled scenes (1000 ms each) were presented which lacked semantic content. The phase-scrambled scenes served as a perceptual baseline. Participants were informed to look at but not remember the phase-scrambled images while maintaining the stimuli presented during the encoding phase, so they also served as interference. For the probe choice task, they were presented with either a new image (negative probe) or a previously presented old image (positive probe), and they had indicated if they saw the image before or not. Participants responded with a fiber optic response pad (fORP, Current Designs, Inc., Philadelphia PA) that was held in their right hand and pressed a green button for Yes and red button for No.

After completing the working memory tasks, an immediate recognition task was completed, which consisted of phase-scrambled images, new images and old images (from L2 and L5). For phase-scrambled images, participants were told just to look at the images and not to make a response. For all other stimuli, participants were told to indicate if the images were new (i.e., never seen before) or old (i.e., from one of the two earlier working memory tasks). The tasks were interspersed with 5-minute rest conditions during which participants fixated on a black cross. The task took approximately 45 minutes to complete, and the total scan time was approximately 90 minutes.

The stimuli were outdoor naturalistic scenes from the SUN database (Xiao et al., 2010) presented at 600 by 800 pixels with a gray background. Images were randomly presented within each trial. The stimuli were presented on an LCD monitor that was located behind the bore of the MRI. Participants had a mirror attached to the head-coil through which they saw the LCD

monitor behind them. Before beginning the task, we confirmed that the participant was able to see the monitor behind them. Participants made responses on a fiber optic box which was placed in their right-hand, equipped with a red and a green button. During the experimental session, participants were not able to see the button box; therefore, they were asked to memorize the location of the buttons and reminded before beginning the task.

2.2 EEG Collection. EEG for both experiments were collected as part of a simultaneous EEG-fMRI experiment. We collected continuous 32-channel passive EEG with Brain Vision MR-Safe caps while simultaneously recording fMRI (31 scalp electrodes and 1 ECG electrode); note, one subject had 64-channel EEG recorded, but for the purpose of comparison with other participants a custom 32-channels montage was applied. This subject was included in all EEG analyses except for the connectivity analysis described below because a custom source montage was unfeasible.. The scalp electrodes were arranged following the 10-10 international system. In accordance with Brain Products simultaneous EEG-fMRI guidelines, AgAL MR-safe gel was used to prepare the caps and all electrode impedanc were brought below 20 k/ohms. The ECG electrode was placed on the back left shoulder blade using the same process. The EEG caps were prepared outside the scanner, impedances were again checked after positioning on the scanner bed and moving into the bore. For safety reasons, impedances were monitored throughout the scanning session, which lasted approximately 2 hours. If impedances went about 35 k/ohm between scans (structural or task), the participant was removed from the bore and the electrode impedance was corrected (Brain Products BrainAmp MR Operating and Reference manual Version 4.0). The participant was repositioned and returned to the bore, impedances were checked before repeating the localizer scan and continuing. No participants were stopped during a task session.

The EEG data was recorded at 2500 Hz and 40 mm caudal to isocenter in the bore of the 3.0 Tesla Siemens scanner (Mullinger et al., 2011). Initially, the first few subjects (n = 5) were recorded at 500 Hz or 1000 Hz and were eventually increased to 2500 Hz to improve fMRI

artifact cleaning. Changes in sampling rate were based on manufacturer recommendations during experimental start-up. After fMRI artifact cleaning was completed, all data was down sampled to 500 Hz.

2.3 EEG Processing. All EEG processing was carried out in BESA Research 7.0. MRI artifact correction was carried out using the BESA Research fMRI artifact gradient removal algorithm with the Allen Method (Allen et al., 2000) following the default BESA settings (number of artifact occurrence averages = 16). This method includes a sliding-window template with 8 artifact occurrences before and after the artifact that are used to create the artifact template, which is then subtracted from the data. The length of each MRI volume was automatically detected (2000 msec) and was based on the user-defined fMRI trigger code recorded during the session (R128) which appeared after 3 dummy scans. For the first 19 participants, the fMRI trigger code was not recorded in the EEG files and was instead substituted with a trigger code recorded in the file (Sync-On, every 2000 ms). In order to align the fMRI gradient artifact with the alternate trigger, the first trigger for each file was manually adjusted in the MRI Artifact Removal settings (i.e., delay between marker volumes and start of volume acquisition).

Ballistocardiogram (BCG) correction was carried out using the ECG electrode channel. For BCG detection, a low cutoff filter of 1 Hz (zero phase, 12dB/oct) and a high cutoff filter of 20 Hz (zero phase, 24 dB/oct) were applied as recommended by BESA Research (BESA Research WIKI, 2020). A template BCG cycle was manually selected for each participant in each file by a trained research assistant. A pattern-matching algorithm was then used to identify the PCA components that explained the BCG pattern (between 4-5 components or whichever variance is less than 1%). Blink correction was carried out using a similar method (Ille et al., 2002; Picton et al., 2000). The method of correction removes the variance associated with a blink (or BCG pattern), from each channel, using the template pattern selected. Blink correction was carried out using the frontal electrodes Fp1 and Fp2 since the EEG-cap did not contain designated electrooculogram channels. Prior to beginning the working memory and recognition tasks,

participants were asked to blink 5-times in a row in order to create a blink-template. If this blink was similar to a spontaneous, this blink was used with a pattern-matching algorithm to identify the PCA component otherwise a more natural blink was selected. If the PCA components accounted for greater than 97% of the variance it was accepted, otherwise the pattern-matching algorithm was run again with another template blink. Artifact-corrected data were used for all analyses in order to ensure that the BCG artifact would not distort the findings. The reference electrode was the frontal pole (Fpz) during recording and was re-referenced offline to the common average reference for sensor-level analyses.

2.4 Time Frequency Analysis. There were 2 WM conditions, low- (2 images) and high-load (5 images) tasks with a same-length delay period (6000 ms). All analyses described below were carried out comparing the low-load delay period with the high-load delay period. Trials were excluded based on BESA Research criteria for artifact rejection: trials were excluded for amplitude > 150 μV, gradient > 75 μV, low-signal criteria > 0.1. In L2, the average number of delay periods was 40 and in L5, it was 42 for each condition, both out of 50 total trials per condition with no difference between conditions ($p = 0.32$).

Time-frequency analysis was carried out at the sensor-level and source-level. Complex demodulation of the recorded EEG signals for each trial was carried out in BESA Research v7.0 (Hoechstetter et al., 2004; Papp & Ktonas, 1977). A detailed description of the demodulation can be found in Ellmore et al. (2017). The timeframe (t) under consideration was the full delay period (0 to 6000 ms) and the baseline was average amplitude across the full epoch (Ellmore et al., 2017). The selected frequency (f) ranges were 4 to 40 Hz: theta (4-8 Hz), alpha (8-13 Hz), and beta (13-30 Hz), and lower gamma (30-40 Hz). Beta is broken down into lower beta (13-20 Hz) and upper beta (20-30 Hz). Time -frequency analysis was generated using the finite impulse response (FIR) filter using latencies of 100 ms and 0.5 Hz frequency steps. The amplitude within each frequency and latency bin was generated for each WM load (termed Time Frequency Amplitude or TFA). TFA is expressed as the absolute value of the amplitude in μV.

The amplitude within a frequency and time bin is the compared to the amplitude of the baseline (termed Temporal Spectral Analysis or TSA). The TSA is expressed as the change in amplitude, either positive or negtive percent change. The equation for TSA is:

$$TSA = \frac{A(t,f) - Abaseline(f)}{Abaseline(f)} * 100\%$$

A(t,f) = amplitude during the timeframe of interest and frequency
$A_{baseline}$ (f) = mean amplitude in the frequency band during the baseline period

If TSA is positive, it reflects synchronization of activity and if it is negative it reflects desynchronization of activity relative to the baseline period (Pfurtscheller, 2001; Pfurtscheller & Da Silva, 1999).

To estimate source-level delay period activity, a default Brain Regions montage was applied to the delay period TSA to account for the potentially overlapping sources of delay activity (Ellmore et al., 2017). The Brain Regions montage is comprised of 15 discrete regions including frontal, temporal, and parietal regions (see *Supplemental Figure 1 and Supplemental Table 2*). The source-level montage estimates the brain region sources by reducing the overlapping signals from the scalp electrodes by calculating weighted combinations of the recorded signal (Hoechstetter et al., 2004; Scherg, 1992). This spatial separation of these fixed ensures that is minimal cross-talk between the regions (Scherg et al., 2019).

2.5 Connectivity and Phase-Locking Analysis. To quantify interaction between brain regions during the delay period, phase-locking value (PLV) analyses were run on the time-frequency data. Both coherence and PLV measure the amount of oscillatory synchronization between two brain regions (Lowet et al., 2016). Coherence is a measure of the linear covariance between two signals in a particular time-frequency bin, taking into account both phase and amplitude of the signal and under the assumption that the signal is stationary in time (Rosenberg et al., 1989). Phase-locking value is a measure of the phase of signal, without respect to the amplitude for a specific frequency-time bin, which is then compared with the

phase of another signal within the same frequency-time (Lachaux et al., 1999). While coherence and phase-locking value may overlap in the connections that are identified, phase-locking value has no assumptions about linearity and stationarity and so it is likely a more robust measure of oscillatory synchronization (Lowet et al., 2016). Moreover, synchrony between two regions only needs to consider the phase of two signals to make determinations about communication (Lachaux et al., 1999). Therefore, in order to make more accurate assumptions about long-range and cross-hemispheric differences, only phase-locking values (PLV) will be compared.

In this analysis, the Brain Regions montage was applied to the data to reduce the number of comparisons. The time frequency analysis was run on the delay period using the same parameters described above; TSA was computed with complex demodulation between 4-40 Hz with 0.5 Hz/100 sec steps, to be consistent with the above analysis. Phase-locking value was computed in BESA Connectivity v 1.0 for both the low- and high-load conditions. For PLV, the values range from 0 (no synchrony) to 1 (completely synchronous) and values between 0-1 represent partial synchrony (Lachaux et al., 1999). The equation for PLV is:

$$PLV_{xy}(f) = \frac{1}{n}\sum_{t=1}^{n} e^{i\cdot(\phi_{xt}-\phi_{yt})}$$

f=frequency of interest, n=number of time points (t) in the epoch, i=imaginary number
ϕ_x and ϕ_x= phase angles from two signals x and y with the frequency of interest

Erroneous results outside the selected frequency range were ignored (BESA Connectivity, 2020). BESA Connectivity data were converted to a BESA Statistics compatible format in Matlab v2020a using BESA generated scripts. 3-D head plots that represent increased connectivity between brain regions were generated in BrainNet Viewer (Xia et al., 2013).

*2.6 Statistical Analysis***.** The behavioral performance on the working memory and immediate recognition tasks were computed using custom Matlab v2020a scripts. Performance is reported as the percent correct out of the total possible trials. Reaction time is reported as the mean reaction time for responses across all trials. Examination of the kurtosis and skewness of

the behavioral performance and reaction time were generated in SPSS v24.0. Non-parametric analysis with related samples Wilcoxon Signed Rank Test were computed after reviewing the skewness and kurtosis of each dependent variable. Regression and pointplots of behavioral performance and mean delay activity in the *Supplemental Results* were run in Python v3.6 using Seaborn v0.11.1.

All delay activity analyses were carried out in BESA Statistics v 2.0, which deals with the multiple comparisons problem by carrying out non-parametric permutation tests produces a cluster value (Maris & Oostenveld, 2007). For the delay activity comparisons across conditions, non-parametric paired t-tests were run. For the correlations with behavior non-parametric correlations were run. A detailed description of the permutation tests can be found in Ellmore et al. (2017). The cluster value is a sum of t- values for a t-test and the cluster value for a correlation is a sum of the r-values for a group of adjacent bins. A bin consists of sensors that are <4 cm distance, latency of 100 msec, and frequency .50 Hz. A null distribution is created by sampling randomly from clusters across subjects and across time-frequency bins. Significant clusters are summed t-, r-, or f-values within a specific time-frequency bin that exceeds a specific threshold and are then compared to the random null distribution created from 1000 permutations (Bullmore et al., 1999; Ernst, 2004; Freedman & Lane, 1983; Maris & Oostenveld, 2007; O'Gorman, 2012). Clusters were considered significant if the p-value was less than or equal to .05.

For the TFA comparisons, significant clusters are indicated with a mask, either blue or orange. An orange cluster represents greater amplitude for one condition versus another (always low-load compared to high-load) for the TFA or event-related synchronization for the TSA. Blue represents a smaller amplitude (for low-load compared to high-load) for the TFA or event-related desynchronization for the TSA. For the connectivity comparisons, significant clusters are also indicated with either blue or red. A red cluster represents greater phase-locking

for one condition versus another (always low-load > high-load) and a blue cluster represents the opposite (greater phase locking for high-load as compared with low-load).

3 Results

3.1 Behavioral. A non-parametric paired samples comparison was conducted on the behavioral measures, as the distributions indicated both moderate skewness and kurtosis. Three subjects were initially included in the behavioral analysis with a large number of no response trials, on either their low- or high-load condition, which were included in the EEG comparisons. These subjects were excluded from the correct trials only analysis (see *Supplemental Results*), so the behavioral analysis was repeated excluding these subjects. Excluding the 3 subjects did not change the behavioral findings, so the results reported below are excluding them. Comparison of performance on the low- and high-load working memory tasks including all subjects revealed a significant short-term difference (*Figure 2)* with better performance on the low-load (mean = 94.74% correct, SD = 6.37) compared to high-load (mean = 86.21% correct, SD = 10.24, related samples Wilcoxon Signed Rank Test p = .001). There was also a long-term advantage of stimuli from the low-load (mean = 70.38% correct, SD = 14.84) as compared with the high-load on the immediate recognition test (mean = 61.43% correct, SD = 17.62, related samples Wilcoxon Signed Rank Test p = .002). Similarly, there was a significant difference for reaction time between the low-and high-load working memory task, with reaction time on the low-load WM task (mean = 878.62 ms, SD = 139.76) faster than the high-load task (mean = 955.71 ms, SD = 122.02, related samples Wilcoxon Signed Rank Test p = .002).

3.2 Correlations with Behavior: Correlations with performance and delay activity were run with corrections for multiple comparisons. The subjects with no responses were excluded from this analysis. There were no significant correlations between TSA delay activity and performance for either condition (L2 p-value = 0.09; L5 p-value = 0.32). There were also no

significant correlations between the phase-locking values (L2 p-value = 0.80; L5 p-value = 0.63) and performance for either condition.

3.3 Absolute Amplitude. Paired-samples t-test with corrections for multiple comparisons were run between the low- and high-load conditions. All subjects were included in this analysis to maximize the signal-to-noise ratio. This sensor-level comparison of the low- and high-load 6-sec delay period revealed 5 significantly different clusters of delay activity (*Table 1*). Four of the five clusters revealed greater amplitude for the low-load condition than the high-load condition throughout the entire delay period (Cluster time = 0-6000 ms) spanning all frequencies. The clusters are mainly in the alpha and beta ranges, with greater amplitude for the low-load compared to the high-load condition (Figure 3a-c). The remaining cluster showed a greater amplitude for the high-load compared to the low load condition in the first half of the delay period (time = 0-2600 ms). This cluster involved right-sided centro-frontal channels (F4'_avr, C4'_avr, FC6'_avr, and CP6'_avr) in the upper beta and gamma range (frequency = 29-37 Hz). This analysis was conducted on all delay period trials, regardless of correct and incorrect probe response. To examine if incorrect responses may have influenced this difference, *Supplemental Figure 1a-d* plots selected significant clusters with performance. This analysis was repeated with delay periods associated with correct probe responses only (see *Supplemental Results*) and the absolute amplitude results remained unchanged.

3.4 Temporal Spectral Amplitude. Paired-samples t-test with corrections for multiple comparisons were run between the low- and high-load conditions. This sensor-level comparison of the low- and high-load 6-sec delay period reveals a transient pattern of delay activity, that is the most pronounced in the right parietal region (Figure 4a-b, P8). Early event-related synchronous (ERS) activity is seen in the alpha and lower beta band, beginning about 1000 ms into the delay and last until about 2000 ms. Event-related desynchronous (ERD) activity is seen in alpha, lower beta, and upper beta beginning about 3500 ms into the delay period and continuing until the end. The pattern of ERS and ERD is more pronounced in the low-load than

the high-load condition but was not significantly different. There was only one cluster of significantly different TSA delay activity. Early in the delay period (time = 300-2500 ms) TSA for the low-load exhibited greater ERD than the high-load condition (Fig 4b-c, cluster value = -1337.84, p = 0.013) specifically in the upper beta and gamma range (frequency = 29.5 – 40 Hz). The significant difference involved 26 of the 31 electrodes across the delay period, with a right lateralized focus.

3.5 Brain Regions Source Montage. In order to make sense of how changes in activity are related to dynamics of these regions (Fries, 2005), namely how these regions are communicating to facilitate maintenance, a source-based brain regions montage was applied to the TSA. The TSA was compared using a paired-samples t-test with corrections for multiple comparisons, and then phase-locking value was generated for each condition and compared. Particularly in time-frequency bins when there are no differences in ERS/ERD, PLV provides insight on if these regions are communicating to facilitate successful maintenance (Fries, 2005; Sauseng et al., 2005).

3.6 Brain Regions-Temporal Spectral Amplitude. Source-level comparison of low- and high-load 6-sec delay period reveals two significantly different clusters of delay activity (Figure 5). The left frontal region exhibited greater event-related synchronization in the low-load as compared with the high-load in the first half of the delay period (Cluster 1: cluster value = 176.60, p = 0.003, frequency = 4-8.5 Hz, greater ERS for L2 time = 2700-3300 ms (FL_BR)). And the left temporoparietal region exhibited greater ERD in the low-load as compared with the high-load condition (Cluster 2: cluster value = -134.03, p = 0.036, frequency = 22.5-27 Hz, greater ERD for L2 time= 1800-2600 msec (TPL_BR) in the early to middle-part of the delay period.

3.7 Brain Regions-Phase Locking Value: Connectivity as measured by phase-locking value for both the low- and high-load appears sustained throughout the entire delay period (*Supplemental Figure 4a and b*). There was increased connectivity between anterior temporal

and temporoparietal regions and parietal regions with both intra-hemispheric (i.e., within the left hemisphere) across all frequency bands and inter-hemispheric connectivity (i.e., across hemispheres) which was restricted to the lower frequency bands. Increased connectivity was observed between central regions (i.e., both midline and bilateral regions) and frontal regions in the upper beta and gamma bands. There was increased connectivity between frontal polar midline and bilateral parietal region in the alpha band. There was also increased connectivity between occipital polar midline and bilateral parietal regions in the gamma and alpha bands.

A paired-samples t-test with corrections for multiple comparisons revealed six significantly different clusters between L2 and L5 (*Table 2*). Red represents greater phase locking in L2 between two regions and blue represents greater phase locking in L5 between two regions. Each PLV connection between brain regions has 2 clusters, one for the feedforward connection and one for the feedback connection. PLV does not provide information on directionality; it just confirms that connectivity could occur in either direction. Only one cluster per connection will be reported here. Fig 6a shows the cluster for the left frontal - right posterior temporal connection (FL_BR - TPR_BR: frequency = 4-9.5 Hz, time range = 0-6000 ms, cluster value = 1120.94, p = 0.024). There was greater phase locking between the left frontal to right posterior temporal regions in the theta and alpha ranges throughout the entire delay period. Fig 6b shows the cluster for the left anterior temporal and left posterior temporal connection (TAL_BR - TPL_BR: frequency = 8.5-18 Hz, time range = 1000-5300 ms, cluster value = 975.11, p = 0.027). There was greater phase locking between the left anterior temporal and left posterior temporal regions in the alpha and lower beta ranges throughout the entire delay period. Fig 6c shows the cluster for the left central - right anterior temporal connection (CL_BR - TAR_BR: frequency = 4-16 Hz, time range = 400-6000 ms, cluster value = 1132.9, p = 0.022). There was greater phase locking between the left central and righter anterior temporal regions in the theta, alpha, and lower beta ranges starting after about 400 ms and continuing until the end of the delay period.

While PLV estimates do not provide directionality between the brain regions, research with primates has suggested that lower frequency oscillations, such as alpha and beta are indicative of feedback connections. Very slow (theta band) and very fast (gamma and high gamma) oscillations are indicative of feedforward connections (Bastos et al., 2015; Miller et al., 2018; Van Kerkoerle et al., 2014). Therefore, these significant clusters potentially reflect mainly feedback connections, although follow-up work using more invasive methods (e.g., intracranial EEG) in humans would need to be done to confirm this.

As stated above this analysis was conducted on all delay period trials, regardless of correct and incorrect probe response. To examine if incorrect responses may have influenced this difference, *Supplemental Figure 3a-f* plots the significant clusters with performance. This analysis was repeated with delay periods associated with correct probe responses only (see *Supplemental Results*). Of the significant clusters discussed above, after repeating the analysis with correct trials only, the significant cluster of PLV between FL – TPR was no longer significant (*Supplemental Figure 5*). The other PLV results remained largely the same and there were 3 additional clusters identified (*Supplemental Figure 6*).

4 Discussion

We hypothesized that if delay activity is a signature of maintenance and attention is crucial for successful maintenance, the introduction of interference will result in reduced delay activity for the low-load condition and have an impact on performance as there were attentional resources available for processing interference. Additionally, there will be reduced frontoparietal connectivity for the low- as compared with the high-load condition. Interestingly, performance was better in the low-load working memory condition as well on the immediate recognition task for stimuli from the low-load condition.

There was greater amplitude in alpha and lower beta bands for the low- compared to the high-working memory load across most sensors. There was also greater amplitude in higher

beta and gamma bands for high- compared to the low-load in right fronto-central sensors in the first half of the delay period. On the sensor-level, both the low- and high-load conditions exhibited transient delay activity. There was an early pattern of event-related synchronization (ERS) in the alpha and low beta regions until about 2000 ms, followed by a pattern of event-related desynchronization (ERD) in the alpha, lower and upper beta regions that started just after the mid-way point until the end of the delay period. These similar transient patterns were not significantly different, with the exception of one cluster of activity. Early in the delay period, greater ERD for low- compared to the high-load in the upper beta and gamma regions across most sensors. When a source-based model was applied to the TSA, differences were found for the left-frontal region in the theta band and very low alpha bands and right-posterior temporal regions in the upper beta band, both in the early-middle delay period.

Both increases in amplitude and ERS in the alpha band are signatures of maintenance that represent inhibition of irrelevant information and brain systems (Jensen & Mazaheri, 2010; Klimesch, 2012). In fact, this may also reflect a period in which knowledge systems, that are accessed automatically when processing stimuli, are inhibited from interfering with the maintained stimuli (Klimesch, 2012). Greater amplitude in the alpha and lower beta range in the low- compared to the high-load condition, could reflect greater disruption of attention for the high-load condition by the interfering stimuli (Bonnefond & Jensen, 2012). It may also reflect the fact that the low-load condition had more resources available to process the interfering stimuli (Yoon et al., 2006); therefore, the available resources were needed to block the interference.. Alternatively, the greater perceptual load of the high-load condition (i.e. five images to maintain plus image complexity) may have resulted in a reduced distractor effect on the delay activity (Lavie et al., 2004).

Event-related desynchronization has also been found in the alpha band during maintenance (Koshy et al., 2020). Decreases in amplitude that are not time-locked (i.e., TSA) to an event have been ascribed to different cognitive processes that can occur during

maintenance. Namely, this pattern of ERD has been associated with manipulation of information held during the delay period (Koshy et al., 2020) as well as the use of cognitive control (Wei & Zhou, 2020). Klimesch et al. (2007) suggested that ERD largely reflects both the anticipation of an upcoming response as well as attentional processes. Additionally, this anticipatory state is a critical time in which semantic information is accessed and supports the maintenance of the complex stimuli (Klimesch, 2012). Lower beta band ERD has also been associated with semantic processing (Hanslmayr et al., 2009), so alpha and low beta band activity may reflect complementary processes (Pavlov & Kotchoubey, 2020). Thus, the ERD observed in the latter half of the delay period of this experiment likely reflects preparation for the upcoming probe-response through an extended period of maintenance (Plaska et al., 2021). As the same type of stimuli were used in both WM conditions this observed pattern of delay activity during the continued period of extended maintenance reflects similar processes regardless of load.

An early period of higher upper beta and gamma band amplitude and ERS was found in the high-load condition compared to the low-load condition with a focus in the right fronto-central regions. Higher beta and gamma activity have been associated with working memory maintenance (Axmacher et al., 2007; Lundqvist et al., 2017; Lundqvist et al., 2016; Palva et al., 2011). In addition to being associated with maintenance, higher beta activity has been associated with volitional control (Lundqvist et al., 2017) and may be related to the selection of which information is maintained (de Vries et al., 2019; de Vries et al., 2020). Gamma increases have also been found to covary with alpha band suppression and are thought to reflect enhanced attentional selection of maintained information (Green et al., 2017). In consideration of the fronto-central location of this difference, control and selection over which information is being maintained (e.g., the encoded stimuli over interfering stimuli) makes sense as the high-load condition likely requires greater control. Alternatively, gamma activity has been associated with processing of attended stimuli in a bottom-up manner (Green et al., 2017; Mazaheri & Jensen, 2010; Sauseng et al., 2008), which would suggest that the interfering stimuli were being

processed during the delay period and could explain the impact on performance. Increases in gamma activity have also been associated with retention of information (Zhao et al., 2017) as well as an anticipatory state during retention prior to using information in working memory (Lundqvist et al., 2017; Miller et al., 2018). While, anticipation of the upcoming probe response is possible for either condition, there would not be an expected difference between these WM loads as the probe response is the same for each condition.

4.1 Connectivity and Maintenance

Increased connectivity was observed between midline frontal and bilateral parietal and central regions during both WM loads. Differences in connectivity between the low- and high-load conditions were found, with greater connectivity between the left central region with right anterior temporal, left frontal and right posterior temporal regions, and left anterior temporal region with the left posterior temporal region. There was increased connectivity between the left central and right anterior temporal region for the low-load condition, in both the analysis of all delay periods and the correct-response delay periods only. The central region represents a superior brain region located near the junction of the frontal and parietal lobes in the left hemisphere, potentially overlapping with the anterior portion of the posterior parietal cortex (Whitlock, 2017). The posterior parietal cortex (PPC) is involved in attentional processes (Hutchinson et al., 2009) with the more dorsal regions associated with allocating attention and control of attention. Increased connectivity between occipital, temporal, and parietal regions such as PPC has been reported with increased WM load. Specifically, increases in lower frequency bands, such as alpha and lower beta, are attributed to deployment of attentional resources (Palva et al., 2010; Palva et al., 2011). Therefore, increased connectivity between left central and right anterior temporal regions within the same frequency bands may reflect control of attention on the maintained stimuli, which was likely easier with 2 images as compared with 5 images, and is critical for preventing the degradation of the WM representation (Lorenc et al., 2021). Alternatively, the left central region may represent part of the phonological – rehearsal

feedback loop as proposed by Buchsbaum and D'Esposito (2019). In this model, the sensorimotor region is connected to the regions involved with carrying out rehearsal (i.e., the anterior temporal region) and provides feedback about the phonological code that is given to the stimuli before covert rehearsal is carried out. In this model, connections with inferior frontal regions are also important for articulation (Buchsbaum & D'Esposito, 2019). Although there was no difference between the loads, there was also increased central – frontal connectivity, which would be consistent with this role in maintenance.

The left frontal region and right posterior temporal region had cross-frequency connectivity in theta, alpha and beta, which may represent both feedforward and feedback connections. Left frontal regions are important for filtering interference and increased attentional selection (Gazzaley & Nobre, 2012; Jha et al., 2004). The right posterior temporal regions may reflect the temporoparietal junction, a critical region for the control of attention (Geng & Vossel, 2013) and may also represent storage of the encoded stimuli (Feredoes et al., 2011; Scheeringa et al., 2009) or selectivity of stimuli into WM (Rezayat et al., 2021). Interestingly, if the posterior temporal region represents a more lateral and inferior temporal region, such as the superior temporal gyrus, this is also consistent with storage of the encoded stimuli. In fact, Park et al. (2011) proposed that the superior temporal gyrus represents the storage place for complex visual stimuli. While filtering is often associated with frontal - parietal connectivity, these connections are established with simple stimuli. Thus, filtering of regions in the brain associated with storage of complex stimuli, such as the stimuli used in this experiment would be essential for successful probe response. Interestingly, the difference in this network emerged only when all trials were included in the analysis and was no longer significant when only examining correct trials. If this network represents filtering of interfering stimuli during the maintenance of complex stimuli then the fact that there was no significant difference between the low- and high-load delay periods (i.e., when looking at correct-response delay periods only) suggests that filtering was critical for successful performance. Therefore, including incorrect

trials in the analysis resulted in disrupted connectivity within this network in the high-load condition and may represent the inability to filter the interference, particularly on the incorrect trials.

Increased frontoparietal connectivity during maintenance is often reported with increasing memory load (Bollinger et al., 2010; Hampson et al., 2006; Payne & Kounios, 2009). We also found increased left frontal to bilateral parietal regions, which could represent filtering of the interfering stimuli, but there was no significant difference between the WM loads. Reduced right-hemisphere frontal-parietal and frontal-midline connectivity has also been reported with increasing set sizes from 2 stimuli to 4 or 6 stimuli (Payne & Kounios, 2009). Payne and Kounios (2009) suggested that reduction in right hemisphere connectivity, particularly in the alpha band, may be a mechanism to prevent interference during maintenance while the left hemisphere activity represented the maintained stimuli. While our results suggest involvement of the same networks and similar frequency bands, we found greater connectivity with frontal regions in the low-load condition. This finding is consistent with the idea that there were more resources available for processing the distractor stimuli in the low-load condition; hence, there was a greater need for continuous filtering throughout the delay period (Yoon et al., 2006). Whereas, in the high-load condition, attentional resources were consumed by the large number of encoded images being maintained, with no resources leftover to processes interfering stimuli (Lavie et al., 2004).

There was also an increase in short-range connectivity between the left anterior temporal region and left temporoparietal region. The left anterior temporal region is critical for language, short-term memory and semantic associations (Boucher et al., 2015; Helmstaedter et al., 1996; Hermann et al., 1992). The left posterior temporal region is a critical junction for somatosensory information and has been implicated in word processing and comprehension (Binder et al., 1997). Phase-locking between these two regions was restricted to the alpha and lower beta regions, which suggests that this connection represents feedback from the anterior

temporal to the posterior region throughout the middle region of the delay period (about 1000-5000 ms). This may represent that process of rehearsal in which the encoded images are recoded into a label and the association of stored semantic knowledge occurs every time the word is rehearsed. Even without explicit instructions to engage in rehearsal, participants are believed to adopt a dual-coding strategy involving verbal recoding and rehearsal, particularly with stimuli that contain high semantic content (Brown et al., 2006) such as the naturalistic scenes used in this task. This increased connectivity was observed in the low-load condition, which represents the fact that it is easier to rehearse two images with word associations than it is for five. In the high-load condition, participants may have had to rely on an alternate maintenance strategy (Chen & Cowan, 2009). If participants relied on an alternate strategy, such as attentional refreshing in the high-load, this may explain the differences in performance. A newly revised model of WM (see Lemaire et al. (2021)) suggests that at higher WM loads, rehearsal is more effective, whereas refreshing alone will result in reduced performance, as was the case in the current experiment.

If increased activity and synchronization is expected with increasing load, as has been reported in many delay period studies (Palva et al., 2010; Zhang et al., 2016), this likely represents that all presented items are being held in working memory (e.g., For a high WM load of 5 stimuli, all 5 stimuli are maintained simultaneously during maintenance). The studies that have established these findings very often use simple stimuli (e.g., colored squares with nameable colors or easy-to-name objects). Therefore, it is possible that reduced amplitude activity and reduced phase-locking for the high-load condition, in the current experiment, could reflect the pattern associated with more complex stimuli such as scenes. In the low-load condition, amplitude and synchronization likely reflects the representation of the two items, no matter how complex, as holding onto two stimuli is well below general working memory capacity (Alvarez & Cavanagh, 2004). On the other hand, the high-load condition is above or near the maximum number of stimuli that can be maintained, although this capacity may differ based on

the individual (Adam et al., 2017). As a result, the maintenance period of the high-load condition may be reduced, both in terms of amplitude activity and connectivity, because participants were not able to maintain all images together. In fact, depending on the individuals' capacity, the maintenance period may only reflect two or three items at a time due to the complex nature, despite the instructions to maintain all images. Both the findings of the planned analysis including all trials and the repeated analysis with correct trials only, are consistent with this possible interpretation.

4.2 Attention and Maintenance

If attention is a fixed resource, the presence of interfering stimuli should consume the available attentional resources needed for maintenance. In fact, since maintaining a higher working memory load requires greater attentional demand than a lower working memory load (5 images versus 2 images), there should be a greater disruption for the higher load (Chen & Cowan, 2009; Wei & Zhou, 2020). This was in fact the case in the comparison of the high- and low-loads for this experiment, as performance was higher on the low-load task. However, participants still performed relatively well on the high-load condition, which suggests that attention wasn't entirely consumed by the interfering stimuli. These results support the fact that attention may not be a fixed resource that is consumed in an all-or-none manner, but rather a flexible resource (Morey et al., 2011). Thus, these results could be explained by the fact that attention could have shifted between maintaining the task stimuli and the interfering stimuli.

Based on task performance, it is clear that attention plays a critical role in maintenance, as interference had a greater impact on the high-load task. However, based on research with different working memory loads, this difference in performance is to be expected without the introduction of interfering stimuli, as there are fewer stimuli to remember. In fact, it could be argued that performance might have been worse on the low-load task since more resources were available to process the interfering stimuli (Lavie, 1995; Lavie & Cox, 1997; Simon et al., 2016). Although, maintenance of more complex stimuli, such as naturalistic scenes, likely

requires an increased need for attentional resources (Chen & Cowan, 2009). Therefore, there may have been no attentional resources leftover to process the interfering stimuli as all of those resources are automatically captured by the complex scenes (Lavie, 1995; Lavie & Cox, 1997; Simon et al., 2016). Complex scenes contain many components, which themselves have features that need to be combined (i.e., palm tree or an ocean), and when combined also have semantic meaning (i.e., a beach). Participants will draw meaningful connections between the stimulus features and that stored knowledge (Asp et al., 2021), which likely requires attentional resources. Thus, even with a low load of only two images, the complexity and associated meaningfulness of the picture may have used up the available resources; thus, the interfering stimuli had no impact on performance.

If sustained attention does not play a role in maintenance, then there should be no difference in frontal region connectivity during maintenance. Frontal-parietal connectivity has been associated with top-down control of attention (Sauseng et al., 2008) and will be differentially engaged based on the attentional requirements. Although the interference in the low- and high-load condition were the same, the required top-down control of attention was different, which was reflected in the different phase-locking for the low- and high load. The low-load condition had greater connectivity between left frontal and right temporal regions throughout the maintenance phase in the theta and alpha bands. Research has found that frontal-parietal synchronization during the delay period of a WM task represents maintenance of information (Salazar et al., 2012). Theta band frontal-parietal synchronization during maintenance has been attributed to both maintenance of information as well as executive attention functions (Sauseng et al., 2008; Sauseng et al., 2005). Thus, the difference in frontal - parietal connectivity reflected the ability to filter out the interfering stimuli and focus on maintenance, which was better in the low-load condition.

4.3 Delay Activity and Interference

External interference has been introduced in working memory tasks in multiple forms, including interfering stimuli that a participant is instructed to ignore as well as a secondary task that occurs during maintenance (Clapp et al., 2010). If the same category distractor is of the same category such as using faces with face distractors, disruption of performance is greater than if the distractor is from a different category, such as faces with scene distractors, and there is a decrease in prefrontal cortex activation (Yoon et al., 2006). The prefrontal cortex (PFC) is a critical frontal region for attention; activation in this region is associated with both filtering out irrelevant information as well as focusing of attention. PFC is both anatomically and functionally linked with parietal regions and involved with attentional control networks (Chadick & Gazzaley, 2011; Gazzaley & Nobre, 2012). Increased activity in parietal regions is also found wjem focusing on task-relevant information (Chadick & Gazzaley, 2011). If the parietal region activation simply reflects storage of visual information, as opposed to attentional processes (Todd & Marois, 2004; Xu & Chun, 2006), it would be expected that activation of this region would have been greater for the high-load condition. However, we found greater parietal activation for the low-load condition, providing additional support for the idea that complex visual stimuli may be stored elsewhere (Park et al., 2011) or more simply reflect that fewer stimuli were maintained during the delay in the high-load condition (e.g., only 2 or 3 images of the 5 presented).

Interestingly, studies with interfering visual stimuli and visual distractors do not show the same resource trade-off that a different domain-distractor might. A possible alternative would be to use a different-domain distractor such as an auditory distractor tone (Morey et al., 2011) that is not related to the working memory task. If the same-domain distractor is from the same-category (i.e. scene stimuli-outdoor with scene stimuli-indoor) it may have had a greater impact on attention (Sreenivasan & Jha, 2007). Interfering stimuli that have similar content, and not just features as the phase-scrambled interfering stimuli did, are more likely to take attentional resources for processing (Yoon et al., 2006). In fact, research with face stimuli and face

distractors as compared with phase-scrambled distractors, have found that only the same-category phase distractors were disruptive to both performance and delay activity (Dolcos & McCarthy, 2006; Dolcos et al., 2007). Alternatively, it is possible that this method of interference was insufficient in capturing attention, in which case a dual-task may have been more appropriate, such as with a judgement task (Clapp et al., 2010), a saccade task (Postle & Hamidi, 2007) or verbal retrieval from a pre-learned word list (Ricker et al., 2010). Future research should examine if different same-category visual stimuli or a dual-task may disrupt attention differently and impact delay activity.

It is also possible that maintenance was protected from interference because participants engaged in maintenance rehearsal. Participants may have automatically recoded the visual stimuli into verbal labels and rehearsed them during maintenance, despite no instructions to do so. In fact, studies have found that the automatic recoding of verbalizable stimuli, such as the naturalistic scenes used in this experiment, will occur even without explicit instructions to do so (Postle et al., 2005). Rehearsal is not an attention-demanding process that will interfere with maintenance of visual information (Vergauwe et al., 2014), but linking semantic associations during rehearsal with visual information which may occur with complex naturalistic scenes (Plaska et al., 2021), may capture attentional resources. If processing and linking of semantic associations occurs during maintenance, then interference may not have occurred because any available attentional resources would be used up and not available to process the distractors. Recently this claim about rehearsal has been revisited with the idea that rehearsal may actually place a demand on attention (Thalmann et al., 2019), which could also explain why the interfering stimuli did not impact performance especially for the low-load condition, when rehearsal is more likely to have been carried out. Future studies should dissociate the attentional demand of rehearsal with complex visual stimuli and the impact of distraction.

4.4 Limitations

This study was collected as part of a simultaneous EEG-fMRI study. The coupling of these powerful imaging techniques provides information about the precise temporal (EEG) and spatial (fMRI) information during maintenance (Cichy & Oliva, 2020). One possible limitation is that EEG collected in the supine condition while laying inside a scanner may show different patterns of amplitude, including reduced cortical activity and laterality differences (Spironelli & Angrilli, 2017). Importantly, the overall cortical patterns observed are consistent with sitting-based EEG (Scheeringa et al., 2009). This should be considered when interpreting the EEG results without the fMRI results. Additionally, to reduce the amount of time spent in the EEG scanner while keeping the number of trials across conditions consistent, the working memory conditions contained only 50 trials each. A larger number of working memory trials per condition may have resulted in better signal-to-noise ratio (Luck, 2014) and enabled a formal comparison between correct and incorrect trials. Finally, this experimental design did not include a control delay period (i.e. blank delay period) in which there were no interfering stimuli present (Postle & Hamidi, 2007). Consequently, it could be argued that the differences in performance and delay activity are simply due to the working memory load difference (2 images vs 5 images) and are unrelated to the interfering stimuli that were originally designed to serve as a perceptual baseline. We argue that this is not the case as the delay activity observed, particularly for the high-load condition, was reduced. With increasing WM load, studies commonly report increased delay activity (Jensen et al., 2002; Jensen & Mazaheri, 2010; Tuladhar et al., 2007). Future studies should include a non-distractor control (i.e., unfilled delay period) to confirm these differences are due to the presence of interfering stimuli.

4.5 Conclusions

The presence of interference during the delay period of a visual working memory task impacted maintenance for complex stimuli. Greater reductions in amplitude were observed in the alpha and beta ranges for the high-load condition suggesting that the presence of visual stimuli during the delay period resulted in a distractor effect. Increased left frontal – right

posterior temporal, left anterior temporal – posterior temporal connectivity, and right anterior temporal - left central connectivity for the low-load condition may explain protection against interference. Successful maintenance of complex visual stimuli in the low-load condition, as evidenced by better performance, is likely the result of attentional filtering of interfering stimuli, the ability to focus attention on maintenance, and the application of verbal maintenance strategies.

References

Adam, K. C., Vogel, E. K., & Awh, E. (2017). Clear evidence for item limits in visual working memory. *Cognitive psychology*, *97*, 79-97.

Allen, P. J., Josephs, O., & Turner, R. (2000). A method for removing imaging artifact from continuous EEG recorded during functional MRI. *NeuroImage*, *12*(2), 230-239.

Alvarez, G. A., & Cavanagh, P. (2004). The capacity of visual short-term memory is set both by visual information load and by number of objects. *Psychological science*, *15*(2), 106-111.

Asp, I. E., Störmer, V. S., & Brady, T. F. (2021). Greater Visual Working Memory Capacity for Visually Matched Stimuli When They Are Perceived as Meaningful. *Journal of Cognitive Neuroscience*, 1-17.

Awh, E., Barton, B., & Vogel, E. K. (2007). Visual working memory represents a fixed number of items regardless of complexity. *Psychological science*, *18*(7), 622-628.

Axmacher, N., Mormann, F., Fernández, G., Cohen, M. X., Elger, C. E., & Fell, J. (2007). Sustained neural activity patterns during working memory in the human medial temporal lobe. *Journal of Neuroscience*, *27*(29), 7807-7816.

Babiloni, C., Babiloni, F., Carducci, F., Cincotti, F., Vecchio, F., Cola, B., Rossi, S., Miniussi, C., & Rossini, P. M. (2004). Functional frontoparietal connectivity during short-term memory as revealed by high-resolution EEG coherence analysis. *Behavioral neuroscience*, *118*(4), 687.

Baddeley, A. (2010). Working memory. *Current biology*, *20*(4), R136-R140.

Baddeley, A. (2012). Working memory: theories, models, and controversies. *Annual review of psychology*, *63*, 1-29.

Baddeley, A. D., & Hitch, G. (1974). Working memory. *Psychology of learning and motivation*, *8*, 47-89.

Bastos, A. M., Vezoli, J., Bosman, C. A., Schoffelen, J.-M., Oostenveld, R., Dowdall, J. R., De Weerd, P., Kennedy, H., & Fries, P. (2015). Visual areas exert feedforward and feedback influences through distinct frequency channels. *Neuron*, *85*(2), 390-401.

BESA Connectivity. (2020). *BESA Connectivity Manual 1.0*.

BESA Research WIKI. (2020). *Pipeline for Simultaneous EEG fMRI*. http://wiki.besa.de/index.php?title=Pipeline_for_simultaneous_EEG-fMRI_recording .

Binder, J. R., Frost, J. A., Hammeke, T. A., Cox, R. W., Rao, S. M., & Prieto, T. (1997). Human brain language areas identified by functional magnetic resonance imaging. *Journal of Neuroscience*, *17*(1), 353-362.

Bollinger, J., Rubens, M. T., Zanto, T. P., & Gazzaley, A. (2010). Expectation-driven changes in cortical functional connectivity influence working memory and long-term memory performance. *Journal of Neuroscience*, *30*(43), 14399-14410.

Bonnefond, M., & Jensen, O. (2012). Alpha oscillations serve to protect working memory maintenance against anticipated distracters. *Current biology*, *22*(20), 1969-1974.

Boucher, O., Dagenais, E., Bouthillier, A., Nguyen, D. K., & Rouleau, I. (2015). Different effects of anterior temporal lobectomy and selective amygdalohippocampectomy on verbal memory performance of patients with epilepsy. *Epilepsy & Behavior*, *52*, 230-235.

Brown, L. A., Forbes, D., & McConnell, J. (2006). Short Article: Limiting the use of Verbal Coding in the Visual Patterns Test. *Quarterly Journal of Experimental Psychology*, *59*(7), 1169-1176.

Buchsbaum, B. R., & D'Esposito, M. (2019). A sensorimotor view of verbal working memory. *Cortex*, *112*, 134-148.

Bullmore, E. T., Suckling, J., Overmeyer, S., Rabe-Hesketh, S., Taylor, E., & Brammer, M. J. (1999). Global, voxel, and cluster tests, by theory and permutation, for a difference between two groups of structural MR images of the brain. *IEEE transactions on medical imaging*, *18*(1), 32-42.

Chadick, J. Z., & Gazzaley, A. (2011). Differential coupling of visual cortex with default or frontal-parietal network based on goals. *Nature neuroscience*, *14*(7), 830-832.

Chen, Z., & Cowan, N. (2009). How verbal memory loads consume attention. *Memory & cognition*, *37*(6), 829-836.

Cichy, R. M., & Oliva, A. (2020). AM/EEG-fMRI Fusion Primer: Resolving Human Brain Responses in Space and Time. *Neuron*.

Clapp, W. C., Rubens, M. T., & Gazzaley, A. (2010). Mechanisms of working memory disruption by external interference. *Cerebral cortex*, *20*(4), 859-872.

Constantinidis, C., Funahashi, S., Lee, D., Murray, J. D., Qi, X.-L., Wang, M., & Arnsten, A. F. (2018). Persistent spiking activity underlies working memory. *Journal of Neuroscience*, *38*(32), 7020-7028.

Coull, J., Frith, C., Frackowiak, R. S. J., & Grasby, P. (1996). A fronto-parietal network for rapid visual information processing: a PET study of sustained attention and working memory. *Neuropsychologia*, *34*(11), 1085-1095.

Cowan, N. (2011). The focus of attention as observed in visual working memory tasks: Making sense of competing claims. *Neuropsychologia*, *49*(6), 1401-1406.

Cowan, N., Elliott, E. M., Saults, J. S., Morey, C. C., Mattox, S., Hismjatullina, A., & Conway, A. R. (2005). On the capacity of attention: Its estimation and its role in working memory and cognitive aptitudes. *Cognitive psychology*, *51*(1), 42-100.

Daume, J., Gruber, T., Engel, A. K., & Friese, U. (2017). Phase-amplitude coupling and long-range phase synchronization reveal frontotemporal interactions during visual working memory. *Journal of Neuroscience*, *37*(2), 313-322.

de Vries, I. E., Savran, E., van Driel, J., & Olivers, C. N. (2019). Oscillatory mechanisms of preparing for visual distraction. *Journal of cognitive neuroscience*, *31*(12), 1873-1894.

de Vries, I. E., Slagter, H. A., & Olivers, C. N. (2020). Oscillatory control over representational states in working memory. *Trends in cognitive sciences*, *24*(2), 150-162.

Dolcos, F., & McCarthy, G. (2006). Brain systems mediating cognitive interference by emotional distraction. *Journal of Neuroscience*, *26*(7), 2072-2079.

Dolcos, F., Miller, B., Kragel, P., Jha, A., & McCarthy, G. (2007). Regional brain differences in the effect of distraction during the delay interval of a working memory task. *Brain research*, *1152*, 171-181.

Ellmore, T. M., Ng, K., & Reichert, C. P. (2017). Early And Late Components Of EEG Delay Activity Correlate Differently With Scene Working Memory Performance. *PLoS One*, *12*(10), e0186072.

Ernst, M. D. (2004). Permutation methods: a basis for exact inference. *Statistical Science*, *19*(4), 676-685.

Fell, J., & Axmacher, N. (2011). The role of phase synchronization in memory processes. *Nature reviews neuroscience*, *12*(2), 105-118.

Feredoes, E., Heinen, K., Weiskopf, N., Ruff, C., & Driver, J. (2011). Causal evidence for frontal involvement in memory target maintenance by posterior brain areas during distracter interference of visual working memory. *Proceedings of the National Academy of Sciences*, *108*(42), 17510-17515.

Freedman, D., & Lane, D. (1983). A nonstochastic interpretation of reported significance levels. *Journal of Business & Economic Statistics*, *1*(4), 292-298.

Fries, P. (2005). A mechanism for cognitive dynamics: neuronal communication through neuronal coherence. *Trends in cognitive sciences*, *9*(10), 474-480.

Gazzaley, A., & Nobre, A. C. (2012). Top-down modulation: bridging selective attention and working memory. *Trends in cognitive sciences*, *16*(2), 129-135.

Gazzaley, A., Rissman, J., & D'esposito, M. (2004). Functional connectivity during working memory maintenance. *Cognitive, Affective, & Behavioral Neuroscience*, *4*(4), 580-599.

Geng, J. J., & Vossel, S. (2013). Re-evaluating the role of TPJ in attentional control: contextual updating? *Neuroscience & Biobehavioral Reviews*, *37*(10), 2608-2620.

Goldman-Rakic, P. S. (1995). Cellular basis of working memory. *Neuron*, *14*(3), 477-485.

Green, J. J., Boehler, C. N., Roberts, K. C., Chen, L.-C., Krebs, R. M., Song, A. W., & Woldorff, M. G. (2017). Cortical and subcortical coordination of visual spatial attention revealed by simultaneous EEG–fMRI recording. *Journal of Neuroscience*, *37*(33), 7803-7810.

Greene, C. M., & Soto, D. (2014). Functional connectivity between ventral and dorsal frontoparietal networks underlies stimulus-driven and working memory-driven sources of visual distraction. *Neuroimage*, *84*, 290-298.

Gruber, O. (2001). Effects of domain-specific interference on brain activation associated with verbal working memory task performance. *Cerebral Cortex*, *11*(11), 1047-1055. https://doi.org/10.1093/cercor/11.11.1047

Gruber, O., & Goschke, T. (2004). Executive control emerging from dynamic interactions between brain systems mediating language, working memory and attentional processes. *Acta psychologica*, *115*(2-3), 105-121.

Hampson, M., Driesen, N. R., Skudlarski, P., Gore, J. C., & Constable, R. T. (2006). Brain connectivity related to working memory performance. *Journal of Neuroscience*, *26*(51), 13338-13343.

Hanslmayr, S., Spitzer, B., & Bäuml, K.-H. (2009). Brain oscillations dissociate between semantic and nonsemantic encoding of episodic memories. *Cerebral cortex*, *19*(7), 1631-1640.

Helmstaedter, C., Elger, C., Hufnagel, A., Zentner, J., & Schramm, J. (1996). Different effects of left anterior temporal lobectomy, selective amygdalohippocampectomy, and temporal cortical lesionectomy on verbal learning, memory, and recognition. *Journal of Epilepsy*, *9*(1), 39-45.

Hermann, B. P., Wyler, A. R., Bush, A. J., & Tabatabai, F. R. (1992). Differential effects of left and right anterior temporal lobectomy on verbal learning and memory performance. *Epilepsia*, *33*(2), 289-297.

Hoechstetter, K., Bornfleth, H., Weckesser, D., Ille, N., Berg, P., & Scherg, M. (2004). BESA source coherence: a new method to study cortical oscillatory coupling. *Brain topography*, *16*(4), 233-238.

Hutchinson, J. B., Uncapher, M. R., & Wagner, A. D. (2009). Posterior parietal cortex and episodic retrieval: convergent and divergent effects of attention and memory. *Learning & Memory*, *16*(6), 343-356.

Ille, N., Berg, P., & Scherg, M. (2002). Artifact correction of the ongoing EEG using spatial filters based on artifact and brain signal topographies. *Journal of clinical neurophysiology*, *19*(2), 113-124.

Jensen, O., Gelfand, J., Kounios, J., & Lisman, J. E. (2002). Oscillations in the alpha band (9–12 Hz) increase with memory load during retention in a short-term memory task. *Cerebral cortex*, *12*(8), 877-882.

Jensen, O., & Mazaheri, A. (2010). Shaping functional architecture by oscillatory alpha activity: gating by inhibition. *Frontiers in human neuroscience*, *4*, 186.

Jensen, O., & Tesche, C. D. (2002). Frontal theta activity in humans increases with memory load in a working memory task. *European journal of Neuroscience*, *15*(8), 1395-1399.

Jha, A. P., Fabian, S. A., & Aguirre, G. K. (2004). The role of prefrontal cortex in resolving distractor interference. *Cognitive, Affective, & Behavioral Neuroscience*, *4*(4), 517-527.

Klimesch, W. (2012). Alpha-band oscillations, attention, and controlled access to stored information. *Trends in cognitive sciences*, *16*(12), 606-617.

Klimesch, W., Sauseng, P., & Hanslmayr, S. (2007). EEG alpha oscillations: the inhibition–timing hypothesis. *Brain research reviews*, *53*(1), 63-88.

Koshy, S. M., Wiesman, A. I., Proskovec, A. L., Embury, C. M., Schantell, M. D., Eastman, J. A., Heinrichs-Graham, E., & Wilson, T. W. (2020). Numerical working memory alters alpha-beta oscillations and connectivity in the parietal cortices. *Human brain mapping*.

Lachaux, J. P., Rodriguez, E., Martinerie, J., & Varela, F. J. (1999). Measuring phase synchrony in brain signals. *Human brain mapping*, *8*(4), 194-208.

Lavie, N. (1995). Perceptual load as a necessary condition for selective attention. *Journal of Experimental Psychology: Human perception and performance*, *21*(3), 451.

Lavie, N. (2005). Distracted and confused?: Selective attention under load. *Trends in cognitive sciences*, *9*(2), 75-82.

Lavie, N., & Cox, S. (1997). On the efficiency of visual selective attention: Efficient visual search leads to inefficient distractor rejection. *Psychological science*, *8*(5), 395-396.

Lavie, N., Hirst, A., De Fockert, J. W., & Viding, E. (2004). Load theory of selective attention and cognitive control. *Journal of experimental psychology: General*, *133*(3), 339.

Lemaire, B., Heuer, C., & Portrat, S. (2021). Modeling Articulatory Rehearsal in an Attention-Based Model of Working Memory. *Cognitive Computation*, 1-20.

Lorenc, E. S., Mallett, R., & Lewis-Peacock, J. A. (2021). Distraction in Visual Working Memory: Resistance is Not Futile. *Trends in cognitive sciences*.

Lowet, E., Roberts, M. J., Bonizzi, P., Karel, J., & De Weerd, P. (2016). Quantifying neural oscillatory synchronization: a comparison between spectral coherence and phase-locking value approaches. *PLoS One*, *11*(1), e0146443.

Luck, S. J. (2014). *An introduction to the event-related potential technique*. MIT press.

Lundqvist, M., Herman, P., Warden, M. R., Brincat, S. L., & Miller, E. K. (2017). Gamma and beta bursts during working memory read-out suggest roles in its volitional control. *bioRxiv*, 122598.

Lundqvist, M., Rose, J., Herman, P., Brincat, S. L., Buschman, T. J., & Miller, E. K. (2016). Gamma and beta bursts underlie working memory. *Neuron*, *90*(1), 152-164.

Mainy, N., Kahane, P., Minotti, L., Hoffmann, D., Bertrand, O., & Lachaux, J. P. (2007). Neural correlates of consolidation in working memory. *Human brain mapping*, *28*(3), 183-193.

Maris, E., & Oostenveld, R. (2007). Nonparametric statistical testing of EEG-and MEG-data. *Journal of neuroscience methods*, *164*(1), 177-190.

Mazaheri, A., & Jensen, O. (2010). Rhythmic pulsing: linking ongoing brain activity with evoked responses. *Front Hum Neurosci*, *4*.

Miller, E. K., Lundqvist, M., & Bastos, A. M. (2018). Working Memory 2.0. *Neuron*, *100*(2), 463-475.

Morey, C. C., & Cowan, N. (2005). When do visual and verbal memories conflict? The importance of working-memory load and retrieval. *Journal of Experimental Psychology: Learning, Memory, and Cognition*, *31*(4), 703.

Morey, C. C., Cowan, N., Morey, R. D., & Rouder, J. N. (2011). Flexible attention allocation to visual and auditory working memory tasks: Manipulating reward induces a trade-off. *Attention, Perception, & Psychophysics*, *73*(2), 458-472.

Mullinger, K. J., Yan, W. X., & Bowtell, R. (2011). Reducing the gradient artefact in simultaneous EEG-fMRI by adjusting the subject's axial position. *NeuroImage*, *54*(3), 1942-1950.

O'Gorman, T. W. (2012). *Adaptive tests of significance using permutations of residuals with R and SAS*. John Wiley & Sons.

Palva, J. M., Monto, S., Kulashekhar, S., & Palva, S. (2010). Neuronal synchrony reveals working memory networks and predicts individual memory capacity. *Proceedings of the National Academy of Sciences*, *107*(16), 7580-7585.

Palva, S., Kulashekhar, S., Hämäläinen, M., & Palva, J. M. (2011). Localization of cortical phase and amplitude dynamics during visual working memory encoding and retention. *Journal of Neuroscience*, *31*(13), 5013-5025.

Papp, N., & Ktonas, P. (1977). Critical evaluation of complex demodulation techniques for the quantification of bioelectrical activity. *Biomedical sciences instrumentation*, *13*, 135.

Park, H., Kang, E., Kang, H., Kim, J. S., Jensen, O., Chung, C. K., & Lee, D. S. (2011). Cross-frequency power correlations reveal the right superior temporal gyrus as a hub region during working memory maintenance. *Brain connectivity*, *1*(6), 460-472.

Pavlov, Y. G., & Kotchoubey, B. (2020). Oscillatory brain activity and maintenance of verbal and visual working memory: A systematic review. *Psychophysiology*, e13735.

Payne, L., & Kounios, J. (2009). Coherent oscillatory networks supporting short-term memory retention. *Brain research*, *1247*, 126-132.

Pfurtscheller, G. (2001). Functional brain imaging based on ERD/ERS. *Vision research*, *41*(10-11), 1257-1260.

Pfurtscheller, G., & Da Silva, F. L. (1999). Event-related EEG/MEG synchronization and desynchronization: basic principles. *Clinical Neurophysiology*, *110*(11), 1842-1857.

Picton, T. W., van Roon, P., Armilio, M. L., Berg, P., Ille, N., & Scherg, M. (2000). The correction of ocular artifacts: a topographic perspective. *Clinical Neurophysiology*, *111*(1), 53-65.

Plaska, C. R., Ng, K., & Ellmore, T. M. (2021). Does rehearsal matter? Left anterior temporal alpha and theta band changes correlate with the beneficial effects of rehearsal on working memory. *Neuropsychologia*, 107825.

Postle, B. R., D'Esposito, M., & Corkin, S. (2005). Effects of verbal and nonverbal interference on spatial and object visual working memory. *Memory & cognition*, *33*(2), 203-212.

Postle, B. R., & Hamidi, M. (2007). Nonvisual codes and nonvisual brain areas support visual working memory. *Cerebral cortex*, *17*(9), 2151-2162.

Rezayat, E., Dehaqani, M.-R. A., Clark, K., Bahmani, Z., Moore, T., & Noudoost, B. (2021). Frontotemporal coordination predicts working memory performance and its local neural signatures. *Nature Communications*, *12*(1), 1103. https://doi.org/10.1038/s41467-021-21151-1

Ricker, T. J., Cowan, N., & Morey, C. C. (2010). Visual working memory is disrupted by covert verbal retrieval. *Psychonomic Bulletin & Review*, *17*(4), 516-521.

Rosenberg, J., Amjad, A., Breeze, P., Brillinger, D., & Halliday, D. (1989). The Fourier approach to the identification of functional coupling between neuronal spike trains. *Progress in biophysics and molecular biology*, *53*(1), 1-31.

Salazar, R., Dotson, N., Bressler, S., & Gray, C. (2012). Content-specific fronto-parietal synchronization during visual working memory. *Science*, *338*(6110), 1097-1100.

SanMiguel, I., Corral, M.-J., & Escera, C. (2008). When loading working memory reduces distraction: behavioral and electrophysiological evidence from an auditory-visual distraction paradigm. *Journal of Cognitive Neuroscience*, *20*(7), 1131-1145.

Sarnthein, J., Petsche, H., Rappelsberger, P., Shaw, G., & Von Stein, A. (1998). Synchronization between prefrontal and posterior association cortex during human working memory. *Proceedings of the National Academy of Sciences*, *95*(12), 7092-7096.

Sauseng, P., Klimesch, W., Gruber, W. R., & Birbaumer, N. (2008). Cross-frequency phase synchronization: a brain mechanism of memory matching and attention. *NeuroImage*, *40*(1), 308-317.

Sauseng, P., Klimesch, W., Schabus, M., & Doppelmayr, M. (2005). Fronto-parietal EEG coherence in theta and upper alpha reflect central executive functions of working memory. *International Journal of Psychophysiology*, *57*(2), 97-103.

Scheeringa, R., Petersson, K. M., Oostenveld, R., Norris, D. G., Hagoort, P., & Bastiaansen, M. C. (2009). Trial-by-trial coupling between EEG and BOLD identifies networks related to alpha and theta EEG power increases during working memory maintenance. *NeuroImage*, *44*(3), 1224-1238.

Scherg, M. (1992). Functional imaging and localization of electromagnetic brain activity. *Brain topography*, *5*(2), 103-111.

Scherg, M., Berg, P., Nakasato, N., & Beniczky, S. (2019). Taking the EEG back into the brain: the power of multiple discrete sources. *Frontiers in neurology*, *10*, 855.

Simon, S. S., Tusch, E. S., Holcomb, P. J., & Daffner, K. R. (2016). Increasing working memory load reduces processing of cross-modal task-irrelevant stimuli even after controlling for task difficulty and executive capacity. *Frontiers in human neuroscience*, *10*, 380.

Smith, E. E., & Jonides, J. (1998). Neuroimaging analyses of human working memory. *Proceedings of the National Academy of Sciences*, *95*(20), 12061-12068.

Sörqvist, P., Dahlström, Ö., Karlsson, T., & Rönnberg, J. (2016). Concentration: The neural underpinnings of how cognitive load shields against distraction. *Frontiers in human neuroscience*, *10*, 221.

Spironelli, C., & Angrilli, A. (2017). Posture used in fMRI-PET elicits reduced cortical activity and altered hemispheric asymmetry with respect to sitting position: an EEG resting state study. *Frontiers in human neuroscience*, *11*, 621.

Sreenivasan, K. K., Curtis, C. E., & D'Esposito, M. (2014). Revisiting the role of persistent neural activity during working memory. *Trends in cognitive sciences*, *18*(2), 82-89.

Sreenivasan, K. K., & D'Esposito, M. (2019). The what, where and how of delay activity. *Nature reviews neuroscience*, 1.

Sreenivasan, K. K., & Jha, A. P. (2007). Selective attention supports working memory maintenance by modulating perceptual processing of distractors. *Journal of cognitive neuroscience*, *19*(1), 32-41.

Sternberg, S. (1966). High-speed scanning in human memory. *Science*, *153*(3736), 652-654.

Thalmann, M., Souza, A. S., & Oberauer, K. (2019). Revisiting the attentional demands of rehearsal in working-memory tasks. *Journal of Memory and Language*, *105*, 1-18.

Todd, J. J., & Marois, R. (2004). Capacity limit of visual short-term memory in human posterior parietal cortex. *Nature*, *428*(6984), 751-754.

Tóth, B., Boha, R., Pósfai, M., Gaál, Z. A., Kónya, A., Stam, C. J., & Molnár, M. (2012). EEG synchronization characteristics of functional connectivity and complex network properties of memory maintenance in the delta and theta frequency bands. *International Journal of Psychophysiology*, *83*(3), 399-402.

Tuladhar, A. M., Huurne, N. t., Schoffelen, J. M., Maris, E., Oostenveld, R., & Jensen, O. (2007). Parieto-occipital sources account for the increase in alpha activity with working memory load. *Human brain mapping*, *28*(8), 785-792.

Van Kerkoerle, T., Self, M. W., Dagnino, B., Gariel-Mathis, M.-A., Poort, J., Van Der Togt, C., & Roelfsema, P. R. (2014). Alpha and gamma oscillations characterize feedback and feedforward processing in monkey visual cortex. *Proceedings of the National Academy of Sciences*, *111*(40), 14332-14341.

Vergauwe, E., Camos, V., & Barrouillet, P. (2014). The impact of storage on processing: How is information maintained in working memory? *Journal of Experimental Psychology: Learning, Memory, and Cognition*, *40*(4), 1072.

Von Stein, A., & Sarnthein, J. (2000). Different frequencies for different scales of cortical integration: from local gamma to long range alpha/theta synchronization. *International Journal of Psychophysiology*, *38*(3), 301-313.

Wei, H., & Zhou, R. (2020). High working memory load impairs selective attention: EEG signatures. *Psychophysiology*, *57*(11), e13643.

Whitlock, J. R. (2017). Posterior parietal cortex. *Current biology*, *27*(14), R691-R695.

Xia, M., Wang, J., & He, Y. (2013). BrainNet Viewer: a network visualization tool for human brain connectomics. *PLoS One*, *8*(7), e68910.

Xiao, J., Hays, J., Ehinger, K. A., Oliva, A., & Torralba, A. (2010). Sun database: Large-scale scene recognition from abbey to zoo. Computer vision and pattern recognition (CVPR), 2010 IEEE conference on,

Xu, Y., & Chun, M. M. (2006). Dissociable neural mechanisms supporting visual short-term memory for objects. *Nature*, *440*(7080), 91-95.

Yoon, J. H., Curtis, C. E., & D'Esposito, M. (2006). Differential effects of distraction during working memory on delay-period activity in the prefrontal cortex and the visual association cortex. *NeuroImage*, *29*(4), 1117-1126.

Zakrzewska, M. Z., & Brzezicka, A. (2014). Working memory capacity as a moderator of load-related frontal midline theta variability in Sternberg task. *Frontiers in human neuroscience*, *8*, 399.

Zhang, D., Zhao, H., Bai, W., & Tian, X. (2016). Functional connectivity among multi-channel EEGs when working memory load reaches the capacity. *Brain research*, *1631*, 101-112.

Zhao, X., Li, X., & Yao, L. (2017). Localized fluctuant oscillatory activity by working memory load: a simultaneous EEG-fMRI study. *Frontiers in behavioral neuroscience*, *11*, 215.

Author Note

Conflict of Interest Statement: The authors declare no competing financial interests

Acknowledgements: We thank A. Duke Shereen, PhD and Kenneth Ng for their help with task set-up and with data collection. We want to thank Farzana Antara, Gabriela Silva, and Albert Perdomo for help with EEG data processing. We also want to thank Michael Epstein, PhD for his constructive feedback on the manuscript.

Funding: This experiment was funded by a CUNY ASRC Seed Grant (Round 4) and NIH R56MH116007.

Disclosure of Interest: The authors report no conflict of interest.

Availability of Data: Deidentified data will be made available upon reasonable request to the corresponding author.

Author Contributions: T.M.E. conceived the experiment and developed the task. C.R.P., J.O., and B.G. carried out EEG-preparation, data collection, and carried out all data processing. C.R.P. carried out all data analysis and wrote the manuscript. J.O. and B.G. reviewed and provided feedback on the manuscript. T.M.E. aided in interpreting the results and writing the manuscript as well as supervised all aspects of the experiment.

Table 1: Significant clusters of absolute amplitude difference between the low- (L2) and high-load (L5) conditions during the delay period (Time: 0 to 6000 msec) for all sensors.

Cluster ID	p-value	Cluster value	Mean for L2 Abs Amp	Mean for L5 Abs Amp	Start Time	End Time	Start Frequency	End Frequency	Electrodes in Cluster
Cluster 1	0.001	25837.9	0.958192	0.761117	0	6000	4	40	F3'_avr, F4'_avr, C3'_avr, C4'_avr, P3'_avr, P4'_avr, O1'_avr, O2'_avr, F8'_avr, T7'_avr, T8'_avr, P7'_avr, P8'_avr, Fz'_avr, Cz'_avr, Pz'_avr, FC1'_avr, FC2'_avr, CP1'_avr, CP2'_avr, FC5'_avr, FC6'_avr, CP5'_avr, CP6'_avr, POz'_avr
Cluster 2	0.016	3093.72	1.17774	0.842218	0	6000	4	20.5	FP1'_avr
Cluster 3	0.016	3046.2	1.23239	0.889094	0	6000	4	18.5	FP2'_avr
Cluster 4	0.044	-905.505	0.439429	0.547827	0	2600	29	37	F4'_avr, C4'_avr, FC6'_avr, CP6'_avr
Cluster 5	0.047	544.782	0.717711	0.630565	2300	5600	19	31.5	TP9'_avr

Table 2: Significant clusters of phase-locking value (PLV) between 15-brain regions during the delay period (Time: 0 to 6000 msec). Each PLV connection between the low- (L2) and high-load (L5) conditions has two significant clusters associated with it to represent the opposite connection (e.g., PL – FL and FL – PL). The PLV results do not provide information about the directionality. The start frequency for all comparisons was 4 Hz, but can erroneously report frequencies lower (i.e., lower than 4 Hz), so start indicates numbers that were adjusted due to erroneous values (see *Methods*).

Cluster ID	p-value	Cluster value	Mean for L2 PVL	Mean for L5 PVL	Start Time	End Time	Start Frequency	End Frequency	Phase-locking Regions
Cluster 1	0.022	1132.9	0.3342	0.223609	400	6000	4*	16	CL_BRtoTAR_BR
Cluster 1	0.022	1132.9	0.3342	0.223609	400	6000	4*	16	TAR_BRtoCL_BR
Cluster 2	0.024	1120.94	0.343857	0.217204	0	6000	4*	9.5	FL_BRtoTPR_BR
Cluster 2	0.024	1120.94	0.343857	0.217204	0	6000	4*	9.5	TPR_BRtoFL_BR
Cluster 3	0.027	975.112	0.346558	0.247562	1000	5300	8.5	18.5	TAL_BRtoTPL_BR
Cluster 3	0.027	975.112	0.346558	0.247562	1000	5300	8.5	18.5	TPL_BRtoTAL_BR

Figure 1. High-load and Low-load Working Memory Task Trial Layout. The task consisted of two working memory loads: a low load (2 images) and a high load (5 images). In the high load condition (top): participants were presented with 5 images in succession (1.4 sec each), a delay period with 6 phase-scrambled images (1 sec per image for a delay period total of 6 sec), a probe choice (1.4 sec), which is either one of the earlier presented images or a new image, and a jitter period with a blank gray screen (approximately 3 sec) that indicates the end of the trial. For the low-load condition (bottom): participants were presented with 2 images in succession (1.4 sec each), a delay period with 6 phase-scrambled images (1 sec per image for a delay period total of 6 sec), a probe choice (1.4 sec), which is either one of the earlier presented images or a new image, and a jitter period with a blank gray screen (approximately 3 sec) that indicates the end of the trial. Participants completed both loads in a randomized order.

Figure 2. Performance on Scene Working Memory Task better for the Low- than the High-Load Condition. Pointplot of performance on the low- (termed: L2) and high-load (termed: L5) WM tasks. Performance was significantly better on the low-load condition as compared with the high-load condition (94.6% correct vs. 86.2%, Wilcoxon Signed Rank Test p = .001). Each color represents an individual subject. Performance accuracy was measured by the percent of trials correct out of the total possible trials. 3 subjects who had a large number of no response trials were excluded.

Figure 3. Comparison of Absolute Amplitude Delay Period Activity in Low-Load and High-Load Conditions Reveals Greater Alpha and Beta Band Amplitude Across the Delay Period. Select absolute amplitude plots in the left frontal and right parietal regions of the 6-sec delay period revealed 5 clusters of significant differences in activity ($p < .05$). Orange clusters represent low-load delay activity greater than high-load and blue clusters represent high-load delay activity greater than low-load. The y-axis shows frequency (Hz); x-axis shows the time in sec. a) Time Frequency Absolute Amplitude plot for the FC6 electrode. The plot shows the low-load condition Absolute Amplitude with the significant clusters overlaid as a mask. b) Head plot of the overall pattern of absolute amplitude difference during the delay period for all sensors. The selected FC6 (Fig 3a) and P3 (Fig 3c) electrodes are highlighted by a dark box on the head plot. c) Time Frequency Absolute Amplitude plot for the P3 electrode. The plot shows the low-load condition Absolute Amplitude with the significant clusters overlaid as a mask.

Figure 4. Comparison of Time Frequency Analysis during Delay in Low-Load and High-Load Conditions Reveals Early Gamma Band ERD. Time Frequency Analysis plot for the P8 electrode during the 6-sec delay period in a whole window analysis. Electrode selected based on results from previous research in our lab highlighting the right parieto-occipital region (Ellmore et al., 2017). a) Time Frequency Analysis for the P8 electrode in the low-load condition. b) Time Frequency Analysis for the P8 electrode in the high-load condition. c) The plot shows the low-load condition Time Frequency Analysis plot from the low-load with the significant cluster overlaid as a mask. The blue cluster represents reduced ERD for the high-load condition. Review of the overall pattern of delay activity during the low- and high-load reveals a similar transient pattern of delay activity for the parieto-occipital censors with an early period of increased synchronous activity in the upper alpha and beta (500 msec to 3000 msec) followed by a period of desynchronous activity in the same frequency bands (4000 msec to 6000 msec).

Figure 5. Delay Period Activity Brain Region Analysis Reveals a Left Posterior Temporal and Left Frontal Regions underly Maintenance. Time Frequency Analysis plots during the 6-sec delay period in a brain regions analysis. The y-axis is frequency (Hz); x-axis is the time in sec. a) 3-D view of Brain Regions Montage superimposed on an MRI structural scan with the Left Posterior Temporal Region highlighted in yellow [left]. Time Frequency Analysis for the Left

Posterior Temporal Region during the 6-sec delay period [right]. The blue cluster represents greater ERD in the upper beta range for the low-load condition. b) 3-D view of Brain Regions Montage superimposed on a template MRI structural scan with the Left Frontal Region highlighted in yellow [left]. Time Frequency Analysis for the Left Frontal during the 6-sec delay period [right]. The red cluster represents greater ERS in the theta and alpha range for the low-load condition.

Figure 6. Phase-locking Value During the Delay Period Reveals 3 Different Connections Supports Maintenance and Reduces Interference in the Low-Load Condition. The plots represent phase-locking (PLV) during the 6-sec delay period in a brain regions connectivity analysis. The y-axis is frequency (Hz); x-axis is the time in sec. 3-D transparent brain frontal (left-top) and left lateral view (left-bottom) displaying the significantly different PLV connections highlighted with a blue connection line. a) Connectivity plot for the low-load condition between left frontal and right posterior temporal regions with mask of significant cluster (right). The significant cluster (red) represents that the low-load condition had greater connectivity between these two regions than the high-load condition ($p = 0.024$). b) Connectivity plot of the significant cluster (red) that represents that the low-load condition had greater connectivity between the left anterior temporal and left posterior temporal regions than the high-load condition ($p = 0.027$). c) Connectivity plot for the low-load condition between right anterior temporal and the left central regions with mask of significant cluster (right). The significant cluster (red) represents that the low-load condition had greater connectivity between these two regions than the high-load condition ($p = 0.022$).

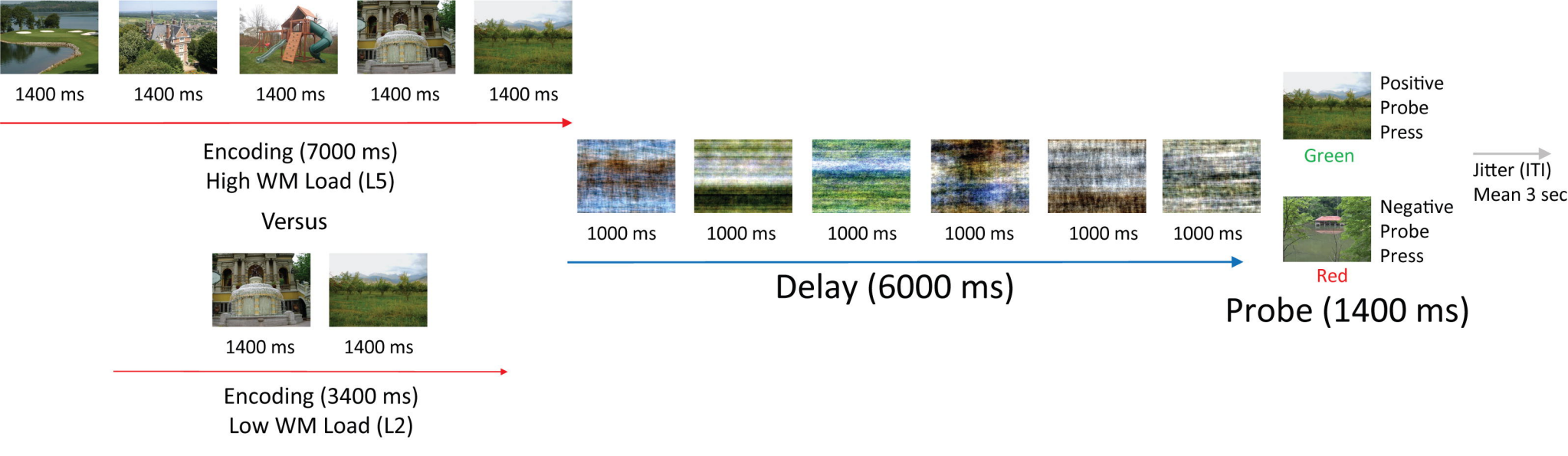
1400 ms
1400 ms
1400 ms
1400 ms
1400 ms
Encoding (7000 ms)
High WM Load (L5)
Versus
1400 ms
1400 ms
Encoding (3400 ms)
Low WM Load (L2)
1000 ms
1000 ms
1000 ms
1000 ms
1000 ms
1000 ms
Delay (6000 ms)
Positive
Probe
Press
Green
Negative
Probe
Press
Red
Probe (1400 ms)
Jitter (ITI)
Mean 3 sec

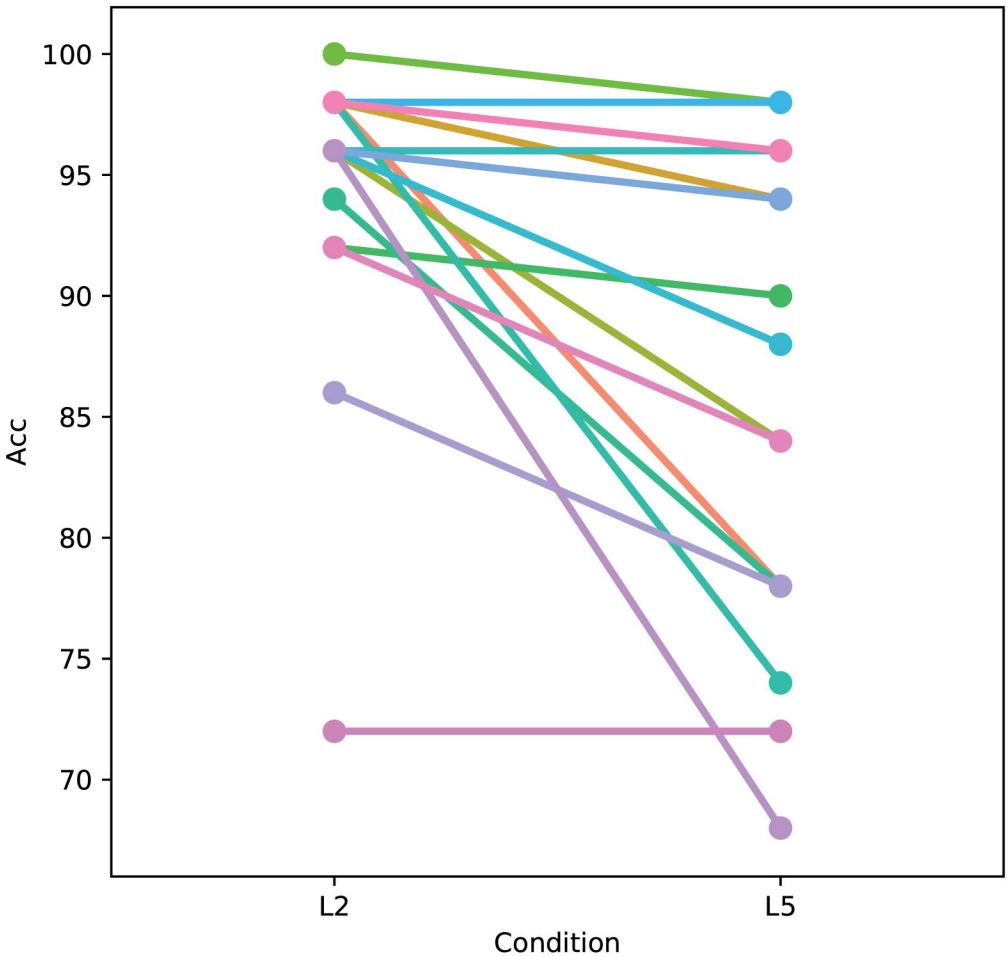
100
95
90
85
80
75
70
Acc
L2
L5
Condition

a) Working Memory Delay Period: FC6 Electrode

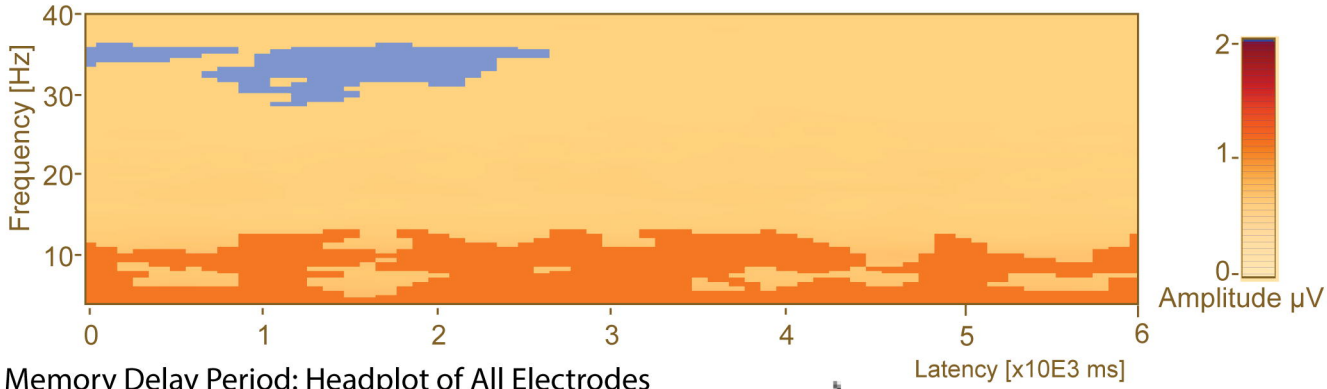

b) Working Memory Delay Period: Headplot of All Electrodes

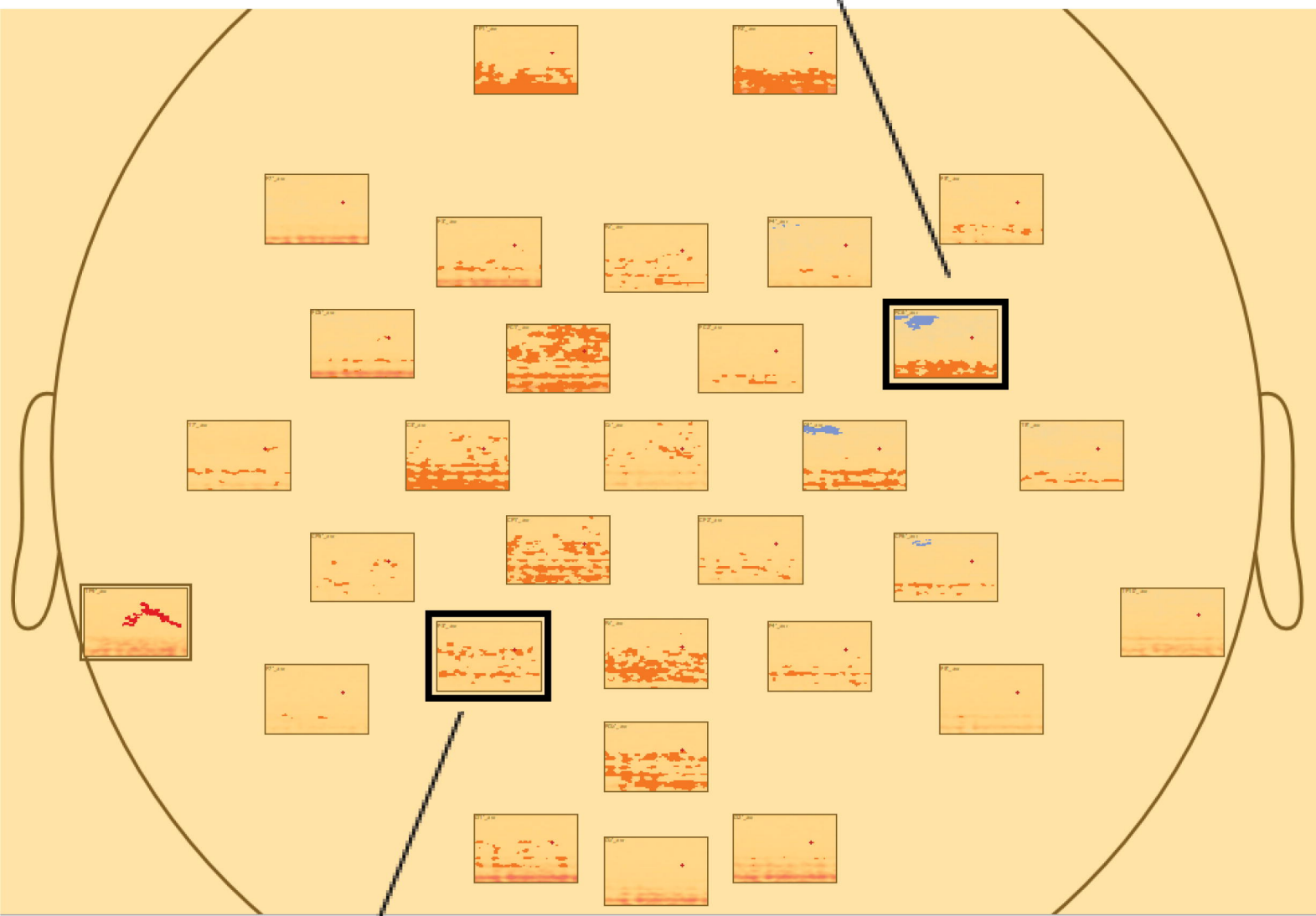

c) Working Memory Delay Period: P3 Electrode

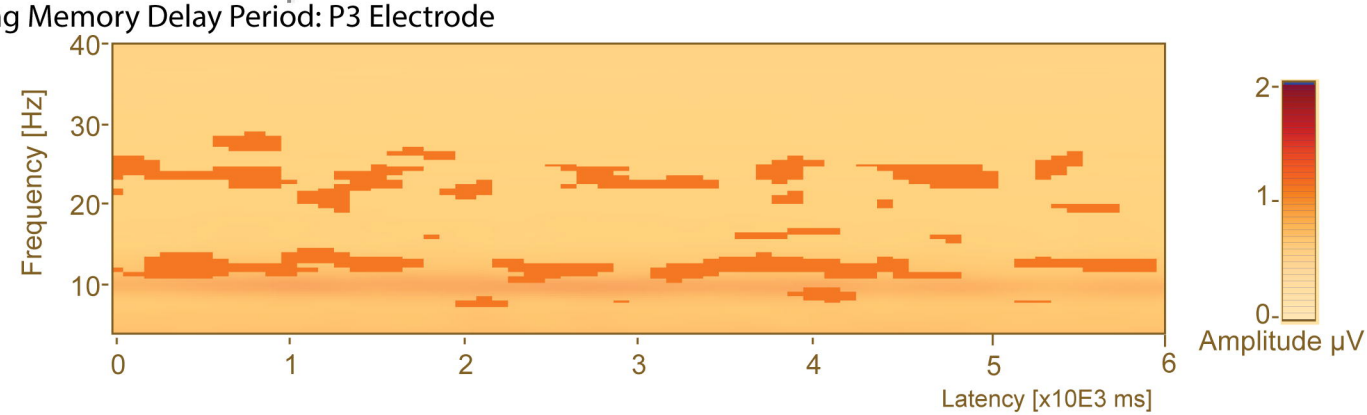

a) Working Memory Load 2

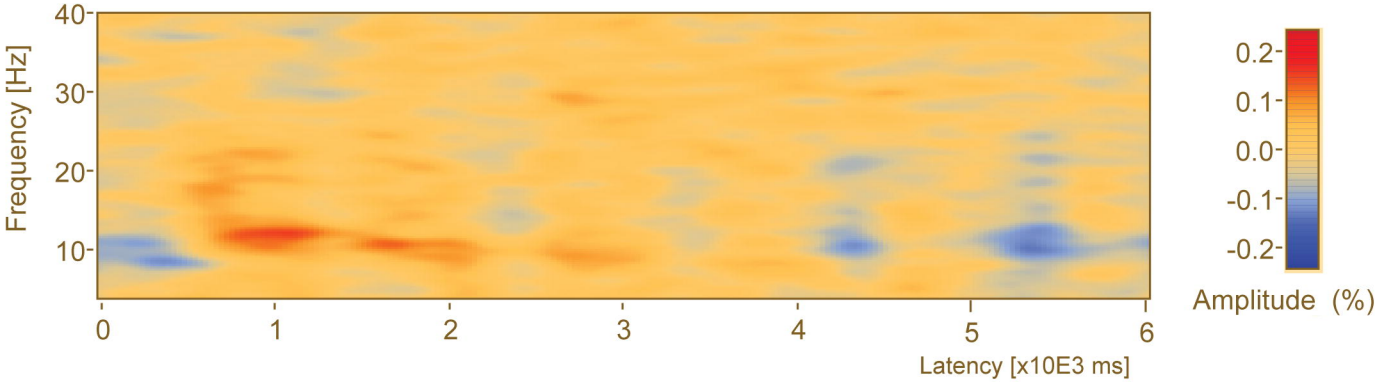

b) Working Memory Load 5

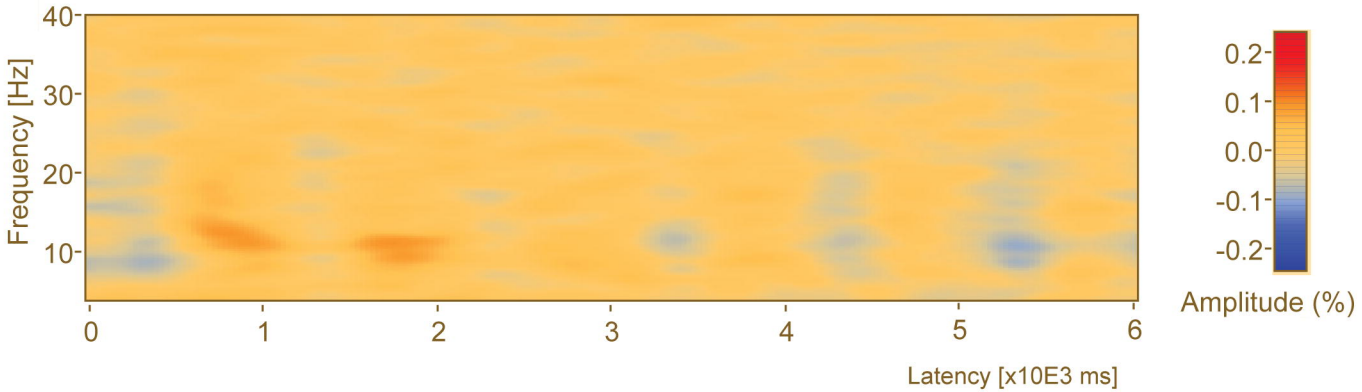

c) Significant Cluster

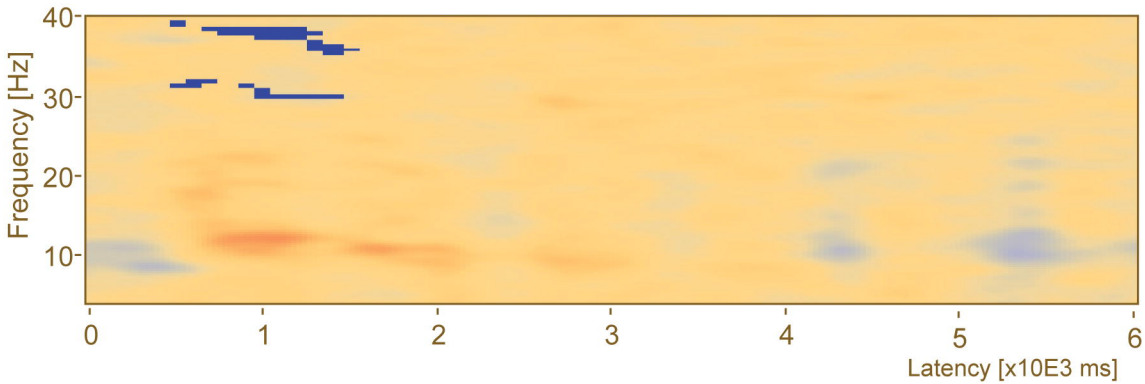

a) Left Posterior Temporal Region

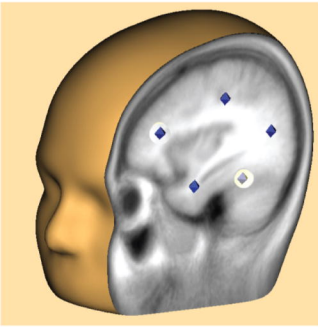

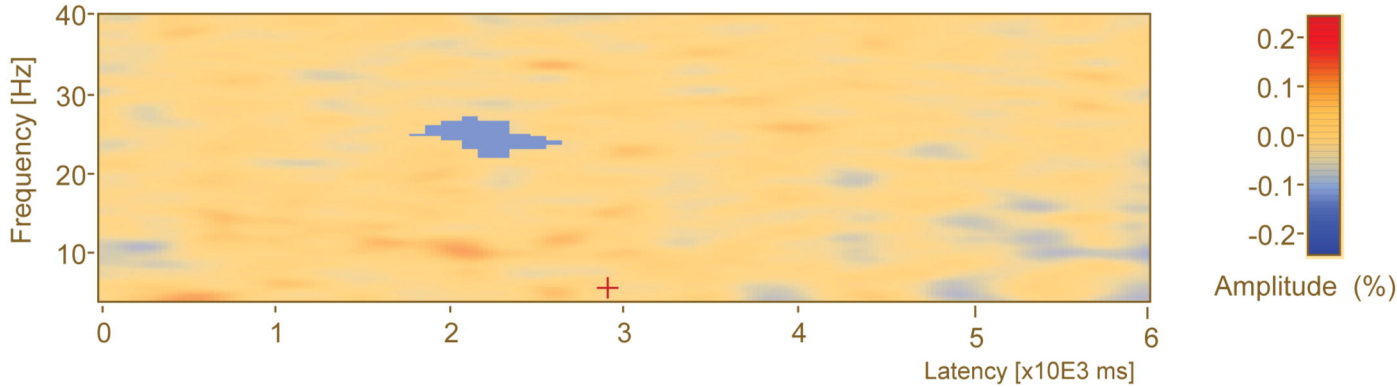

b) Left Frontal Region

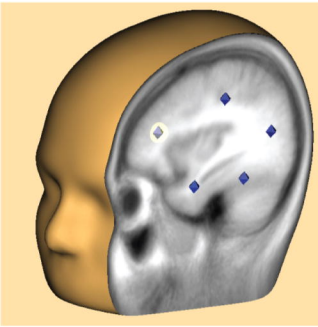

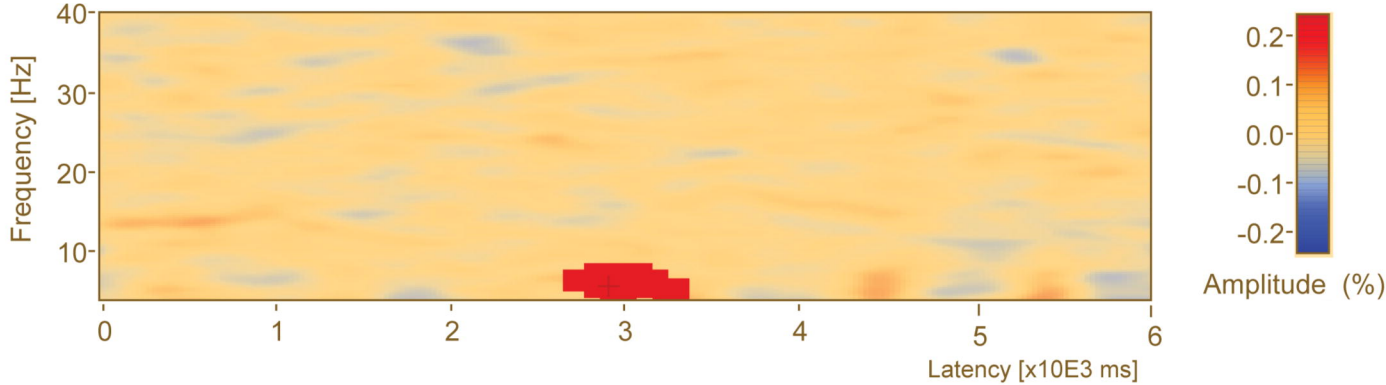

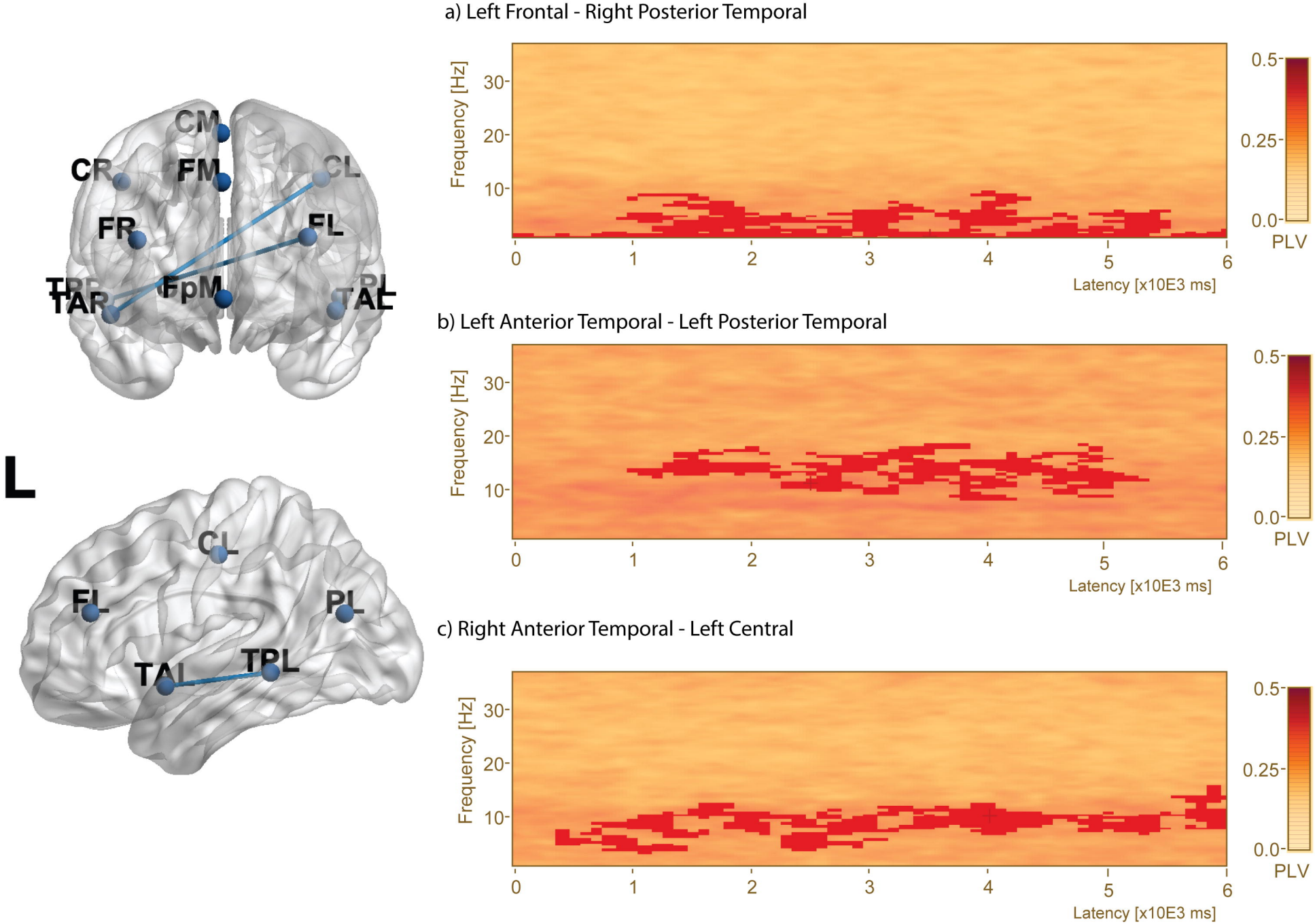
a) Left Frontal - Right Posterior Temporal
b) Left Anterior Temporal - Left Posterior Temporal
c) Right Anterior Temporal - Left Central
CM
CR
FM
CL
FR
FL
FpM
TAR
TAL
L
CL
FL
PL
TAL
TPL
Frequency [Hz]
Latency [x10E3 ms]
PLV
0.5
0.25
0.0
10
20
30
0
1
2
3
4
5
6